

POP-Pincer Silyl Complexes of Group 9: Rhodium versus Iridium

Miguel A. Esteruelas,* Montserrat Oliván, and Andrea Vélez

Departamento de Química Inorgánica, Instituto de Síntesis Química y Catálisis Homogénea (ISQCH), Universidad de Zaragoza - CSIC, 50009 Zaragoza, Spain

Supporting Information

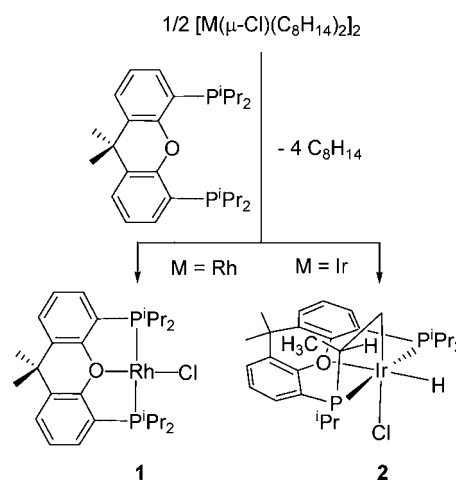
ABSTRACT: 9,9-Dimethyl-4,5-bis(diisopropylphosphino)-xanthene ($\text{xant}(\text{P}^i\text{Pr}_2)_2$) derivatives $\text{RhCl}\{\text{xant}(\text{P}^i\text{Pr}_2)_2\}$ (**1**) and $\text{IrHCl}\{\text{xant}(\text{P}^i\text{Pr}_2)_2\}[\text{PrPCH}(\text{Me})\text{CH}_2]$ (**2**) react with diphenylsilane and triethylsilane to give the saturated d^6 compounds $\text{RhHCl}(\text{SiR}_3)\{\text{xant}(\text{P}^i\text{Pr}_2)_2\}$ ($\text{SiR}_3 = \text{SiHPh}_2$ (**3**), SiEt_3 (**4**)) and $\text{IrHCl}(\text{SiR}_3)\{\text{xant}(\text{P}^i\text{Pr}_2)_2\}$ ($\text{SiR}_3 = \text{SiHPh}_2$ (**5**), SiEt_3 (**6**)). Complexes **3** and **5** undergo a Cl/H position exchange process via the $\text{MH}\{\text{xant}(\text{P}^i\text{Pr}_2)_2\}$ ($\text{M} = \text{Rh}$ (**8**), Ir (**E**)) intermediates. The rhodium complex **3** affords the square planar d^8 -silyl derivative $\text{Rh}(\text{SiClPh}_2)\{\text{xant}(\text{P}^i\text{Pr}_2)_2\}$ (**7**), whereas the iridium derivative **5** gives $\text{IrH}_2(\text{SiClPh}_2)\{\text{xant}(\text{P}^i\text{Pr}_2)_2\}$ (**9**), which is stable. In agreement with the formation of **7**, the reactions of **8** with silanes are a general method to prepare square planar d^8 -rhodium-silyl derivatives. Thus, the addition of triethylsilane and triphenylsilane to **8** initially leads to the dihydrides $\text{RhH}_2(\text{SiR}_3)\{\text{xant}(\text{P}^i\text{Pr}_2)_2\}$ ($\text{SiR}_3 = \text{SiEt}_3$ (**10**), SiPh_3 (**11**)), which lose molecular hydrogen to afford $\text{Rh}(\text{SiR}_3)\{\text{xant}(\text{P}^i\text{Pr}_2)_2\}$ ($\text{SiR}_3 = \text{SiEt}_3$ (**12**), SiPh_3 (**13**)). Treatment of **7** with $\text{NaBAR}_4 \cdot 2\text{H}_2\text{O}$ leads to the cationic five-coordinate d^6 -species $[\text{RhH}\{\text{Si}(\text{OH})\text{Ph}_2\}\{\text{xant}(\text{P}^i\text{Pr}_2)_2\}]\text{BAR}_4$ (**14**) through a silylene intermediate. According to the participation of the latter in the formation of **14**, this cation is an efficient catalyst precursor for the monoalcoholysis of diphenylsilane with a wide range of alcohols, reaching turnover frequencies at 50% of conversion between 4000 and 76 500 h^{-1} . The X-ray structures of **3**, **6**, **7**, **9**, **12**, and **14** are also reported.

INTRODUCTION

Complexes containing diphosphine pincer ligands are attracting increased interest because their high stability and disposition of the donor atoms allow them to develop a marked ability to form less common coordination polyhedra and favor unusual metal oxidation states.¹ Thus, in the search for new transition-metal catalysts, more robust than those based on *trans*- $\text{M}(\text{P}^i\text{Pr}_3)_2$ metal fragments, we synthesized the ligands 9,9-dimethyl-4,5-bis(diisopropylphosphino)xanthene ($\text{xant}(\text{P}^i\text{Pr}_2)_2$) and 4,6-bis(diisopropylphosphino)dibenzofuran ($\text{dbf}(\text{P}^i\text{Pr}_2)_2$) three years ago.² These diphosphines were subsequently used to prepare POP-complexes of Os(II), Os(III), Os(IV), and Os(VI), some of which proved to be promising alternatives to ruthenium for the direct synthesis of imines from alcohols and amines, with liberation of molecular hydrogen,³ and for the regioselective head-to-head (*Z*)-dimerization of terminal alkynes.⁴ We have recently widened our work to rhodium and iridium. Thus, following the previously developed methodology to access the chemistry of the *trans*- $\text{Rh}(\text{P}^i\text{Pr}_3)_2$ and *trans*- $\text{Ir}(\text{P}^i\text{Pr}_3)_2$ metal fragments, we performed the reactions of the dimers $[\text{M}(\mu\text{-Cl})(\text{C}_8\text{H}_{14})_2]_2$ ($\text{M} = \text{Rh}, \text{Ir}$) with $\text{xant}(\text{P}^i\text{Pr}_2)_2$ that afforded the square planar rhodium(I) derivative $\text{RhCl}\{\text{xant}(\text{P}^i\text{Pr}_2)_2\}$ (**1**)⁵ and the iridium(III) complex $\text{IrHCl}\{\text{xant}(\text{P}^i\text{Pr}_2)_2\}[\text{PrPCH}(\text{Me})\text{CH}_2]$ (**2**) in high yields (Scheme 1).⁶ Now, we have investigated the reactivity of **1** and **2** toward silanes.

Reactions of transition-metal complexes with silanes are of great current interest due to the relevance of M-SiR_3 intermediates⁷ in transition-metal catalyzed processes such as

Scheme 1

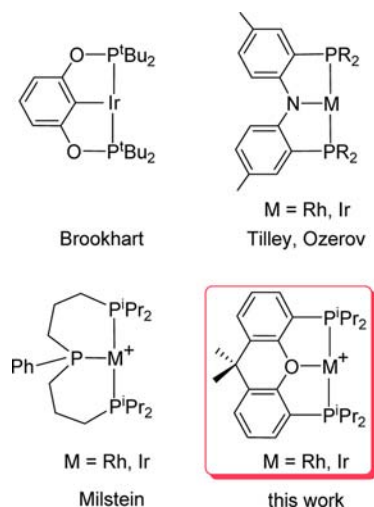


the hydrosilylation of unsaturated organic substrates,⁸ the direct synthesis of chlorosilanes,⁹ and Si-H/OH coupling.¹⁰ Silyl complexes containing pincer diphosphine ligands are very rare, in particular for rhodium and iridium. The linker groups encountered consist of either metalated aryl or amide units in anionic POCOP or PNP ligands or neutral PP_2 triphosphines (Chart 1). Brookhart¹¹ has studied the mechanism of (POCOP) IrH_2 -catalyzed reduction of a variety of tertiary

Received: July 26, 2013

Published: October 2, 2013

Chart 1

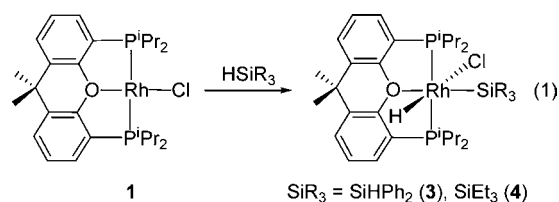


amides with H_2SiEt_2 (POCOP = 2,6-bis(di-*tert*-butylphosphinito)phenyl) and established that the neutral silyl trihydride Ir(V) complex $(\text{POCOP})\text{IrH}_3(\text{SiH}_2\text{Et}_2)$ is the catalytically active species, whereas the highly electrophilic η^1 -silyl derivative $[(\text{POCOP})\text{IrH}(\eta^1\text{-HSiEt}_3)]^+$ catalyzes the hydrosilylation of ketones, aldehydes, esters, epoxides, allyl halides, and ethers. Tilley¹² has described synthetic pathways to a variety of (PNP)Ir–silyl and –silylene complexes (PNP = bis(*o*-diisopropylphosphinophenyl)amide) and explored the catalytic activation of the silylene species in the silane alcoholysis and aminolysis and for the hydrosilylation of ketones and alkenes. Ozerov¹³ has provided insight into the relative thermodynamic affinity of the (PNP)Rh skeleton toward the oxidative addition of various halosilanes and how it compares with its affinity toward addition of other species. Milstein¹⁴ has reported on the synthesis of rhodium and iridium complexes containing the triphosphine ligand $^i\text{Pr}_2\text{P}(\text{CH}_2)_3\text{P}(\text{Ph})(\text{CH}_2)_3\text{P}^i\text{Pr}_2$ (PP_2) and described their reactivity toward $\text{HSi}(\text{SEt})_3$.

This paper reports on the similarities and differences in the behavior of the metal fragments $\text{Rh}\{\text{xant}(\text{P}^i\text{Pr}_2)_2\}$ and $\text{Ir}\{\text{xant}(\text{P}^i\text{Pr}_2)_2\}$ toward silanes and on the catalytic activity of the five-coordinate d^6 -complex $[\text{RhH}\{\text{Si}(\text{OH})\text{Ph}_2\}\{\text{xant}(\text{P}^i\text{Pr}_2)_2\}]\text{BAR}^{\text{F}}_4$ in the monoalcoholysis of diphenylsilane.

RESULTS AND DISCUSSION

Saturated d^6 -Hydride-silyl Complexes. The square planar rhodium(I) complex $\text{RhCl}\{\text{xant}(\text{P}^i\text{Pr}_2)_2\}$ (**1**) oxidatively adds the Si–H bond of silanes. Thus, at room temperature, the treatment of toluene solutions of this compound with 1.1 equiv of diphenylsilane and triethylsilane leads to the saturated d^6 -hydride-silyl derivatives $\text{RhHCl}(\text{SiR}_3)\{\text{xant}(\text{P}^i\text{Pr}_2)_2\}$ ($\text{SiR}_3 = \text{SiHPh}_2$ (**3**), SiEt_3 (**4**)), which were isolated as white solids in 81% (**3**) and 56% (**4**) yield, according to eq 1.



Complex **3** was characterized by X-ray diffraction analysis. Figure 1 gives a view of its structure. As expected for a pincer

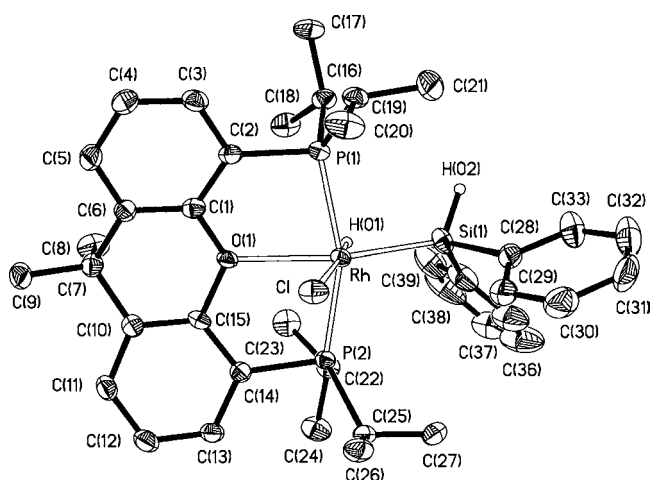


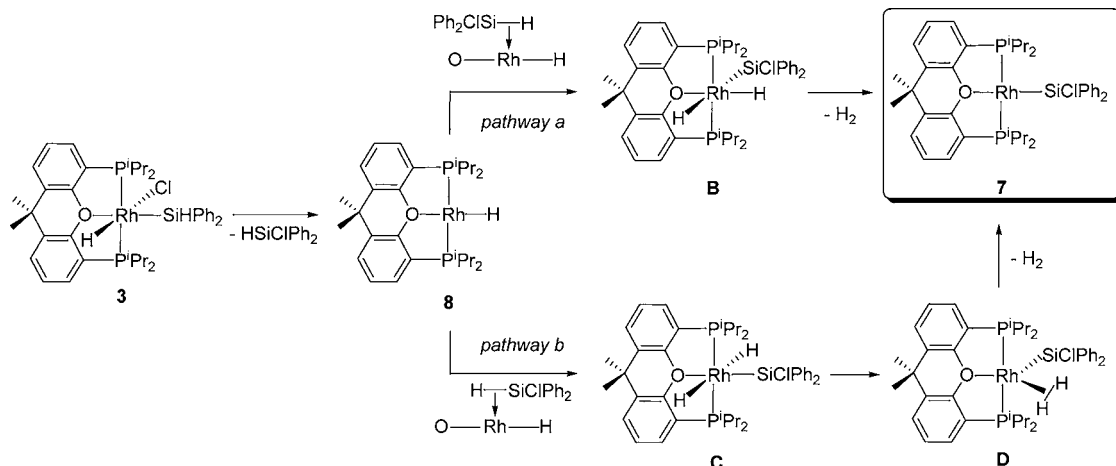
Figure 1. ORTEP diagram of complex **3** (50% probability ellipsoids). Hydrogen atoms (except hydride and Si–H) are omitted for clarity. Selected bond lengths (Å) and angles (deg): Rh–Cl = 2.4367(9), Rh–P(1) = 2.2885(9), Rh–P(2) = 2.3046(9), Rh–Si(1) = 2.2660(10), Rh–O(1) = 2.384(2); P(1)–Rh–P(2) = 160.27(3), P(1)–Rh–O(1) = 80.83(6), P(2)–Rh–O(1) = 79.58(6), Si(1)–Rh–O(1) = 158.32(6).

coordination of the diphosphine, the Rh(POP) skeleton is T-shaped with the rhodium atom situated in the common vertex and P(1)–Rh–P(2), P(1)–Rh–O(1), and P(2)–Rh–O(1) angles of 160.27(3)°, 80.83(6)°, and 79.58(6)°, respectively. So, the coordination geometry around the metal center can be rationalized as a distorted octahedron with the silyl group *trans*-disposed to the oxygen atom of the diphosphine (Si(1)–Rh–O(1) = 158.32(6)°) and the hydride *trans*-disposed to the chloride ligand. This ligand disposition is consistent with a concerted *cis*-addition of the Si–H bond along the O–Rh–Cl axis of **1** with the silyl group directed toward the chloride ligand.¹⁵ The Rh–Si bond length of 2.2660(10) Å compares well with Rh(III)–Si single bond distances previously reported.¹⁶

The ^1H , $^{31}\text{P}\{^1\text{H}\}$, and $^{29}\text{Si}\{^1\text{H}\}$ NMR spectra of **3** and **4**, in benzene- d_6 , at room temperature are consistent with the structure shown in Figure 1. Thus, the ^1H NMR spectra show hydride resonances at –15.90 (**3**) and –16.29 (**4**) ppm which appear as double triplets with H–Rh and H–P coupling constants of about 24 and 15 Hz, respectively. In agreement with equivalent P^iPr_2 groups, the $^{31}\text{P}\{^1\text{H}\}$ NMR spectra contain at 42.9 (**3**) and 41.6 (**4**) ppm doublets with P–Rh coupling constants of 112 and 120 Hz, respectively. In the $^{29}\text{Si}\{^1\text{H}\}$ NMR spectra, the silyl groups display at 4.1 (**3**) and 40.3 (**4**) ppm double triplets with Si–Rh and Si–P coupling constants of 36 and 13 Hz (**3**) and 32 and 11 Hz (**4**).

Iridium is more reducing than rhodium and shows higher tendency to form coordinatively saturated compounds.^{6,17} As a consequence, the iridium dimer $[\text{Ir}(\mu\text{-Cl})(\text{C}_8\text{H}_{14})_2]_2$ reacts with $\text{xant}(\text{P}^i\text{Pr}_2)_2$ to afford the saturated d^6 complex **2** (Scheme 1). However, the latter undergoes demetalation by reductive elimination to act as a synthon of the unsaturated d^8 species $\text{IrCl}\{\text{xant}(\text{P}^i\text{Pr}_2)_2\}$ (**A**),⁶ the iridium(I) counterpart of **1**. Thus, at room temperature, the treatment of toluene solutions of **2** with 1.1 equiv of diphenylsilane and triethylsilane affords $\text{IrHCl}(\text{SiR}_3)\{\text{xant}(\text{P}^i\text{Pr}_2)_2\}$ ($\text{SiR}_3 = \text{SiHPh}_2$ (**5**), SiEt_3 (**6**)), the

Scheme 3

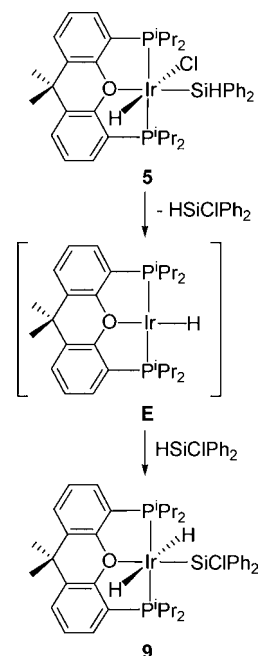


reaction given the *cis*-orientation of the hydride ligands and the marked preference of the $\text{Rh}\{\text{xant}(\text{P}^i\text{Pr}_2)_2\}$ skeleton for the unsaturated d^8 species. However, the *trans*-disposition of the hydride ligands in C prevents the three-centered transition state for their reductive elimination. So, the loss of molecular hydrogen requires the previous dissociation of the oxygen atom of the diphosphine, which should become bidentate.²¹ The dissociation of the oxygen atom of the diphosphine should allow the formation of the dihydrogen intermediate or transition state D, which could easily give 7.

Complex 5, the iridium counterpart of 3, is also unstable in solution. In toluene at 50 °C, it evolves into the *trans*-dihydride $\text{IrH}_2(\text{SiClPh}_2)\{\text{xant}(\text{P}^i\text{Pr}_2)_2\}$ (9) that is the iridium counterpart of intermediate C (Scheme 3). The transformation is quantitative after 2 days, as judged by ^1H and $^{31}\text{P}\{^1\text{H}\}$ NMR spectroscopy. The formation of 9 can be rationalized in a similar manner to that of C via a square planar iridium(I) monohydride intermediate $\text{IrH}\{\text{xant}(\text{P}^i\text{Pr}_2)_2\}$ (E), analogous to 8, which should be generated by reductive elimination of HSiClPh_2 . Thus, the subsequent oxidative addition of the H–Si bond of the formed silane along the O–Ir–H axis of E with the silyl group directed toward the hydride ligand could afford the *trans*-dihydride (Scheme 4). In favor of this proposal, we have observed that the addition of 2.0 equiv of diphenylsilane to a benzene- d_6 solution of 6 in an NMR tube at 50 °C affords 9, via 5, and HSiEt_3 . In this context, it should be noted that complex 9 is more stable than 5 in spite of the destabilization produced by the strong *trans* influence of the hydride ligands mutually *trans* disposed.²² This fact is consistent with density functional theory (DFT) calculations on the model complexes $\text{Os}(\text{SiR}_3)\text{Cl}(\text{CO})(\text{PH}_3)_2$ ($\text{R} = \text{F}, \text{Cl}, \text{OH}, \text{Me}$), which have revealed that a linear combination of Si–R σ^* orbitals is responsible for some π -acceptor capacity of the silyl group. This component increases its contribution to the bond as the electronegativity of the substituent at the silicon atom also increases.²³ The difference in behavior between rhodium and iridium in this Cl/H position exchange process agrees well with the higher preference of iridium for the saturated d^6 species.^{6,17}

The *trans*-dihydride 9 was isolated as a white solid in 60% yield and characterized by X-ray diffraction analysis. An ORTEP drawing of the molecule is shown in Figure 4. The structure proves the Cl/H position exchange and the *trans* disposition of the hydride ligands ($\text{H}(01)\text{--Ir--H}(02) = 173(3)^\circ$). The coordination polyhedron around the iridium

Scheme 4



atom can be rationalized as a distorted octahedron with the diphosphine *mer*-coordinated ($\text{P}(1)\text{--Ir--P}(2) = 159.01(4)^\circ$, $\text{P}(1)\text{--Ir--O} = 81.04(7)^\circ$, $\text{P}(2)\text{--Ir--O} = 80.77(7)^\circ$) and the silyl group *trans* disposed to the oxygen atom of the diphosphine ($\text{Si--Ir--O} = 167.72(7)^\circ$). The Ir–Si bond length of 2.2655(11) Å compares well with that of 6.

The ^1H , $^{31}\text{P}\{^1\text{H}\}$, and $^{29}\text{Si}\{^1\text{H}\}$ NMR spectra in benzene- d_6 at room temperature, are consistent with the structure shown in Figure 4. In agreement with the presence of *trans*-hydrides, the ^1H NMR spectrum shows at -4.90 ppm a triplet with a H–P coupling constant of 16.6 Hz. As expected for equivalent P^iPr_2 groups, the $^{31}\text{P}\{^1\text{H}\}$ NMR spectrum contains at 47.9 ppm a singlet. The silyl group displays at -4.8 ppm a triplet with a Si–P coupling constant of 20 Hz in the $^{29}\text{Si}\{^1\text{H}\}$ NMR spectrum.

Square-Planar Rhodium(II)-silyl Complexes. The formation of 7 according to Scheme 3 suggested that the monohydride 8 should be an efficient starting material to prepare square planar rhodium(II)-silyl derivatives in a general manner. The addition of 1.1 equiv of triethylsilane and

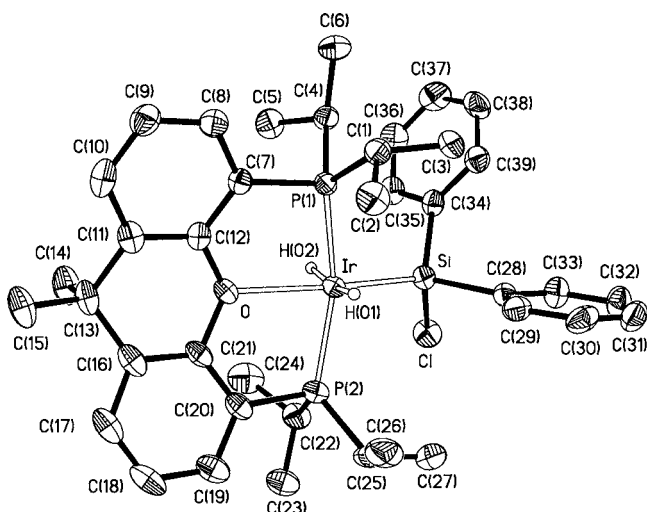
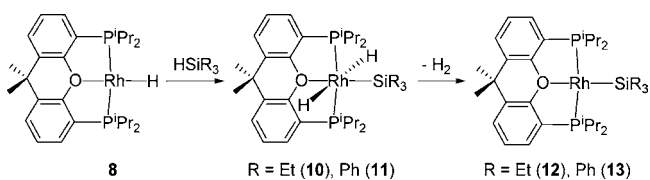


Figure 4. ORTEP diagram of complex **9** (50% probability ellipsoids). Hydrogen atoms (except hydrides) are omitted for clarity. Selected bond lengths (Å) and angles (deg): Ir–P(1) = 2.2811(10), Ir–P(2) = 2.2704(10), Ir–Si = 2.2654(11); P(1)–Ir–P(2) = 159.01(4), P(1)–Ir–O = 81.04(7), P(2)–Ir–O = 80.77(7), Si–Ir–O = 167.72(7), H(01)–Ir–H(02) = 173(3).

triphenylsilane to the toluene solutions of **8** leads to the *trans*-dihydride derivatives $\text{RhH}_2(\text{SiR}_3)\{\text{xant}(\text{P}^i\text{Pr}_2)_2\}$ ($\text{SiR}_3 = \text{SiEt}_3$ (**10**), SiPh_3 (**11**)), which release molecular hydrogen to afford the rhodium(I) complexes $\text{Rh}(\text{SiR}_3)\{\text{xant}(\text{P}^i\text{Pr}_2)_2\}$ ($\text{SiR}_3 = \text{SiEt}_3$ (**12**), SiPh_3 (**13**)). The reductive elimination of molecular hydrogen could take place in a similar manner to those shown in Scheme 3 or via a protonation–dehydrogenation mechanism, as reported by Brookhart for a related PNP–Ir system,²⁴ catalyzed by traces of H_2O . The trend of **10** and **11** to lose molecular hydrogen is in contrast with the behavior of **4** and $\text{RhH}_2\text{Cl}\{\text{xant}(\text{P}^i\text{Pr}_2)_2\}$ and consistent with the inertness of the monohydride **8** toward molecular hydrogen.⁶

Scheme 5



The dihydride intermediates **10** and **11** were spectroscopically detected and fully characterized when the reactions were performed in a NMR tube at 258 K. Their ^1H NMR spectra show at -5.63 (**10**) and -5.02 (**11**) ppm double triplets, with H–Rh and H–P coupling constants of 17.6 and 18.0 (**10**) Hz and 19.3 and 16.1 (**11**) Hz, corresponding to the hydride ligands. The $^{31}\text{P}\{^1\text{H}\}$ NMR spectra contain at 61.6 (**10**) and 59.3 (**11**) ppm doublets with Rh–P coupling constants of 126 and 120 Hz, respectively. The silyl groups display at 33.0 (**10**) and 9.4 (**11**) ppm double triplets, with Si–Rh and Si–P coupling constants of 33 and 9 (**10**) Hz and 42 and 12 (**11**) Hz, in the $^{29}\text{Si}\{^1\text{H}\}$ NMR spectra.

The square planar complexes **12** and **13** were isolated as red solids in a 58% and 81% yield, respectively. The triethylsilyl derivative **12** was characterized by X-ray diffraction analysis. Figure 5 shows an ORTEP drawing of the molecule. Like for **7**, the coordination geometry around the rhodium atom is almost

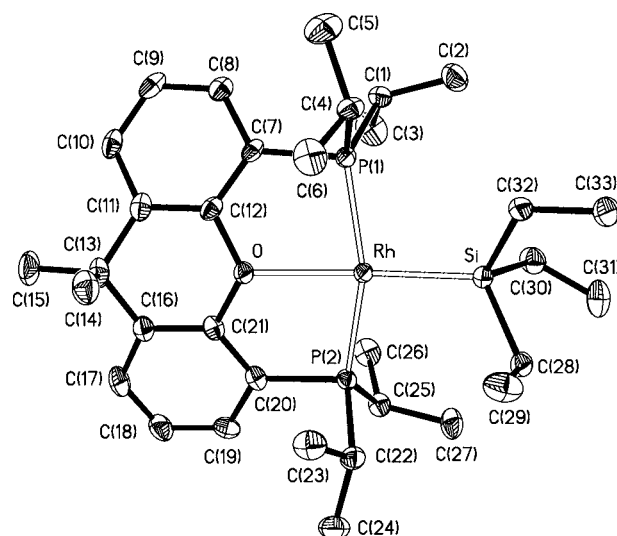


Figure 5. ORTEP diagram of complex **12** (50% probability ellipsoids). Hydrogen atoms are omitted for clarity. Selected bond lengths (Å) and angles (deg): Rh–P(1) = 2.2541(8), Rh–P(2) = 2.2573(8), Rh–Si = 2.3090(8), Rh–O = 2.3149(18); P(1)–Rh–P(2) = 158.51(3), P(1)–Rh–O = 81.39(5), P(2)–Rh–O = 81.57(5), Si–Rh–O = 170.0(5).

square planar with the diphosphine coordinated in a *mer*-fashion (P(1)–Rh–(2) = 158.51(3)°, P(1)–Rh–O = 81.39(5)°, P(2)–Rh–O = 81.57(5)°) and the silyl group *trans* disposed to the oxygen atom of the diphosphine (Si–Rh–O = 170.0(5)°). In this case, the greatest deviation from the best plane through the rhodium, silicon, P(1), oxygen, and P(2) atoms is 0.1198(4) Å for Rh. The Rh–Si bond length of 2.3090(8) Å compares well with that of **7**. In agreement with Figure 5, the $^{31}\text{P}\{^1\text{H}\}$ NMR spectra of **12** and **13** contain at 46.0 and 44.7 ppm doublets with P–Rh coupling constants of 171 and 159 Hz, respectively, whereas the $^{29}\text{Si}\{^1\text{H}\}$ NMR spectra show at 25.0 (**12**) and 14.4 (**13**) ppm double triplets with Si–Rh and Si–P coupling constants of 54 and 19 (**12**) Hz and 66 and 21 (**13**) Hz.

Catalytic Monoalcoholysis of Ph_2SiH_2 . The square planar rhodium(I) complex **7** is the entry to an interesting rhodium(III)-silyl species. Treatment of its fluorobenzene solutions with 1.2 equiv of $\text{NaBAR}^{\text{F}}_4 \cdot 2\text{H}_2\text{O}$ ($\text{Ar}^{\text{F}} = 3,5$ -bis(trifluoromethyl)phenyl), at room temperature, for 1 h results in chloride abstraction from the silyl group and the formation of the five-coordinate hydride-silyl derivative $[\text{RhH}\{\text{Si}(\text{OH})\text{Ph}_2\}\{\text{xant}(\text{P}^i\text{Pr}_2)_2\}]\text{BAR}^{\text{F}}_4$ (**14**). Its formation can be rationalized according to Scheme 6. The chloride abstraction should initially afford the silylene intermediate **F**, which could subsequently undergo the heterolytic addition of an O–H bond of water to give the hydride-silyl derivative.

Complex **14** was isolated as a white solid in 76% yield and characterized by X-ray diffraction analysis. The structure proves its formation. Figure 6 shows a view of the cation of the salt. The geometry around the rhodium atom can be described as a distorted trigonal bipyramid with the P^iPr_2 groups of the pincer in apical positions (P(1)–Rh–P(2) = 157.16(3)°, P(1)–Rh–O(1) = 83.47(5)°, P(2)–Rh–O(1) = 84.13(5)°) and inequivalent angles within the Y-shaped equatorial plane (O(1)–Rh–Si = 138.62(5)°, O(1)–Rh–H(01) = 156.0(12)°, and Si–Rh–H(01) = 65.3(12)°). The Rh–Si bond length of 2.3000(8) Å is about 0.03 Å longer than that of the saturated rhodium(III) derivative **3**. In agreement with the

Scheme 6

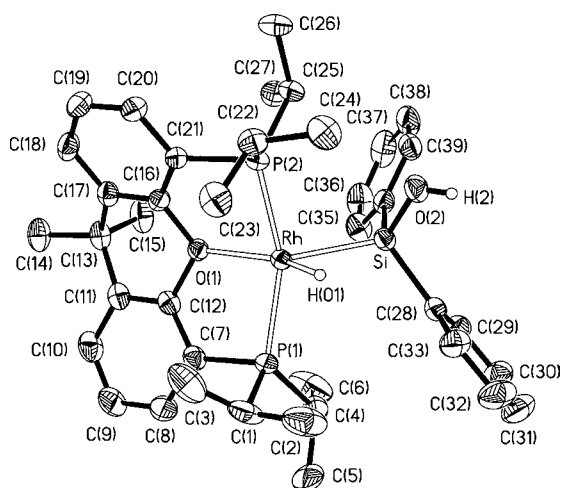
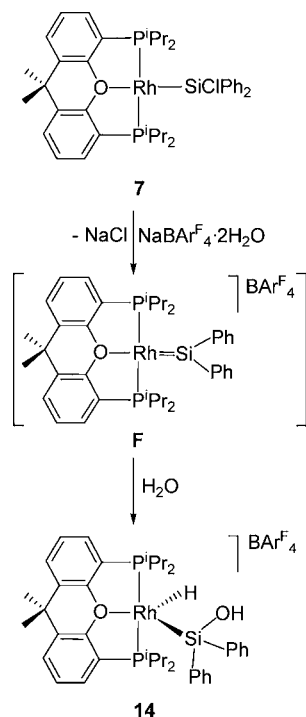


Figure 6. ORTEP diagram of the cation of complex **14** (50% probability ellipsoids). Hydrogen atoms (except hydride and O–H) are omitted for clarity. Selected bond lengths (Å) and angles (deg): Rh–P(1) = 2.3165(7), Rh–P(2) = 2.2794(7), Rh–Si = 2.3000(8), Rh–O(1) = 2.1859(17); P(1)–Rh–P(2) = 157.16(3), P(1)–Rh–O(1) = 83.47(5), P(2)–Rh–O(1) = 84.13(5), O(1)–Rh–Si = 138.62(5), Si–Rh–H(01) = 65.3(12), O(1)–Rh–H(01) = 156.0(12).

presence of the hydride ligand, the ¹H NMR spectrum, in dichloromethane-*d*₂, at 233 K shows at –17.43 ppm a double triplet with H–Rh and H–P coupling constants of 39.4 and 12.5 Hz, respectively, whereas the OH- resonance appears at 3.25 ppm as a broad singlet. As expected for equivalent PⁱPr₂ groups coordinated to a Rh(III) center, the ³¹P{¹H} NMR spectrum at 233 K contains at 52.1 ppm a doublet with a P–Rh coupling constant of 119 Hz. The silyl group displays at 26.1 ppm a double triplet with Si–Rh and Si–P coupling constants of 32 and 7 Hz, respectively, in the ²⁹Si{¹H} NMR spectrum at 233 K.

Tilley has demonstrated that iridium-silylene complexes are active catalyst for the alcoholysis of silanes.^{12c} This prompted us to investigate the alcoholysis of the diphenylsilane promoted by **14** (eq 2), since its formation seems to take place through the silylene intermediate **F**. The reactions were performed in toluene at 32 °C, using 0.17 mol % of catalyst and silane and alcohol concentrations of 0.3 M. Under these conditions, alkoxy silanes HSi(OR)Ph₂ were selectively formed in quantitative yield, after seconds or a few minutes, with spectacularly high turnover frequencies at 50% conversion (TOF_{50%}), which range from 4000 to 76 500 h⁻¹, and isolated in high yields between 71% and 92% (Table 1).

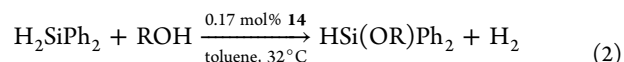


Table 1. Monoalcoholysis of H₂SiPh₂ Catalyzed by [RhH{Si(OH)Ph₂}{xant(PⁱPr₂)₂}]BAr^F₄ (**14**)^a

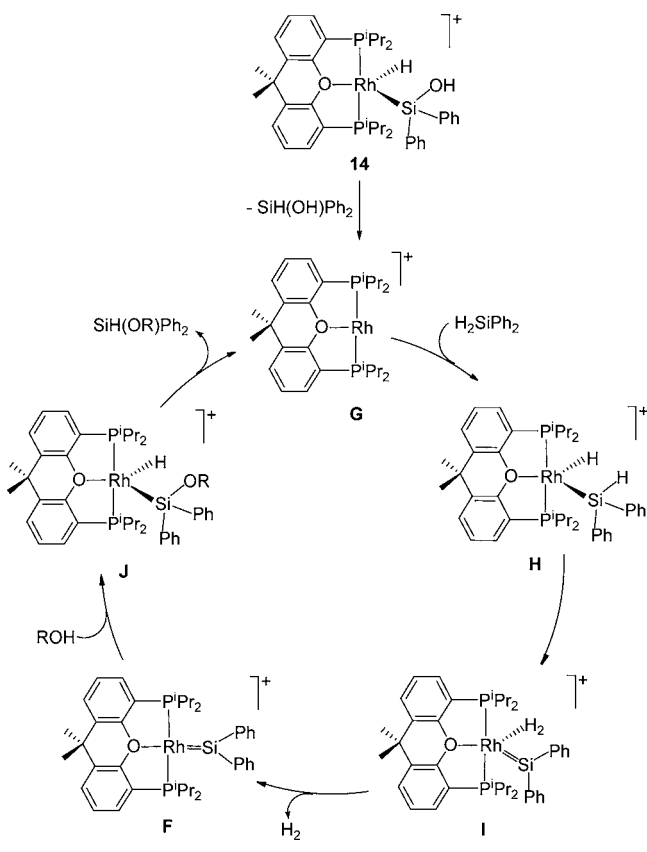
Run	Alcohol	Product	TOF _{50%} (h ⁻¹)	Isolated yield (%)
1	methanol		25300	89
2	ethanol		44000	87
3	1-butanol		53000	83
4	1-octanol		63600	71
5	benzyl alcohol		25000	71
6	2-propanol		76500	92
7	cyclohexylalcohol		62800	75
8	<i>t</i> -butanol		18000	81
9	phenol		4000	72

^a0.17 mol % **14**, 0.3 M H₂SiPh₂, 0.3 M alcohol in toluene (5 mL) at 32 °C. Turnover frequencies [(mol product/mol Rh)/time] were calculated at 50% conversion.

Primary, secondary, and tertiary alcohols, as well as phenol were successfully used. For primary alcohols, the reaction rates increase as the length of the carbon chain increases, that is, in the sequence methanol (run 1) < ethanol (run 2) < 1-butanol (run 3) < 1-octanol (run 4). The secondary alcohols 2-propanol (run 6) and cyclohexanol (run 7) yield the corresponding alkoxy silanes with TOF_{50%} values similar or higher than 1-octanol. Although the reactions with the tertiary *t*-butanol (run 8) and with phenol (run 9) are also very efficient, these substrates afford the lowest TOF_{50%} values, 18 000 h⁻¹ and 4000 h⁻¹, respectively.

The selective monoalcoholysis of the silane is notable and fully consistent with the participation of a silylene species as key

Scheme 7



intermediate of the process. The nucleophilic attack of the alcohol to an η^2 -silane complex, $M(\eta^2\text{-H-SiR}_3)$, has been considered an alternative manner of generating silylethers.²⁵ However, such possibility cannot justify the selectivity observed in this case. Furthermore, it should imply the heterolytic cleavage of the H–Si bond, which should require an electrophilic metal center, and this does not seem to be the case of Rh(I).²⁶ It should be also noted that in contrast to standard methods involving the treatment of silylchloride with an alcohol in the presence of a base that generates hydrochloride salts byproducts,²⁷ this process is environmentally benign and occurs with liberation of molecular hydrogen.

The catalysis can be rationalized according to Scheme 7. The reductive elimination of HSi(OH)Ph_2 from **14** could initially afford the rhodium(I) intermediate **G**, which should oxidatively add diphenylsilane to give **H**. Thus, the elimination of molecular hydrogen from the latter through **I** could lead to the silylene **F**, which should form **J** in a similar manner as **14**. Then, the reductive elimination of the alkoxy silane from **J** could generate **G** again.

CONCLUDING REMARKS

This study has revealed that the square planar d^8 -complexes $\text{MCl}\{\text{xant}(\text{P}^i\text{Pr}_2)_2\}$ ($\text{M} = \text{Rh}, \text{Ir}$) oxidatively add the Si–H bond of tertiary and secondary silanes, along the O–M–Cl axis with the silyl group directed toward the chloride ligand, to give d^6 -chloro-hydride-silyl derivatives $\text{MHCl}(\text{SiR}_3)\{\text{xant}(\text{P}^i\text{Pr}_2)_2\}$ and $\text{MHCl}(\text{SiHR}_2)\{\text{xant}(\text{P}^i\text{Pr}_2)_2\}$. Complexes containing secondary silyl groups undergo a Cl/H position exchange to afford dihydride-chlorosilyl compounds $\text{MH}_2(\text{SiClR}_2)\{\text{xant}(\text{P}^i\text{Pr}_2)_2\}$, through Cl–SiHR₂ reductive elimination and subsequent H–

SiClR₂ oxidative addition to $\text{MH}\{\text{xant}(\text{P}^i\text{Pr}_2)_2\}$ intermediates. According to the higher oxidizing character of the 4d metals, the rhodium species lose molecular hydrogen and, as a consequence, the addition of the H–Si bond of silanes to the square planar monohydride complex $\text{RhH}\{\text{xant}(\text{P}^i\text{Pr}_2)_2\}$ leads to square planar d^8 -silyl compounds $\text{Rh}(\text{SiR}_3)\{\text{xant}(\text{P}^i\text{Pr}_2)_2\}$, in a general manner, through the corresponding d^6 intermediates $\text{MH}_2(\text{SiR}_3)\{\text{xant}(\text{P}^i\text{Pr}_2)_2\}$. Interestingly, the abstraction of chloride from $\text{Rh}(\text{SiClPh}_2)\{\text{xant}(\text{P}^i\text{Pr}_2)_2\}$ in the presence of water yields the five-coordinate d^6 -species $[\text{RhH}\{\text{Si(OH)Ph}_2\}\{\text{xant}(\text{P}^i\text{Pr}_2)_2\}]^+$, as a result of the addition of an O–H bond of water to the Rh–Si double bond of a silylene intermediate. In agreement with the participation of the latter in the formation of this cationic compound, it is a very efficient catalyst precursor for the selective monoalcoholysis of diphenylsilane that reaches turnover frequencies (TOF) at 50% of conversion up to $76\,500\text{ h}^{-1}$.

In conclusion, the $\text{Rh}\{\text{xant}(\text{P}^i\text{Pr}_2)_2\}$ metal fragment favors unsaturated d^8 -square planar, $\text{Rh}(\text{SiR}_3)\{\text{xant}(\text{P}^i\text{Pr}_2)_2\}$, and d^6 -five coordinate, $[\text{RhH}\{\text{Si(OH)Ph}_2\}\{\text{xant}(\text{P}^i\text{Pr}_2)_2\}]^+$, silyl complexes whereas the $\text{Ir}\{\text{xant}(\text{P}^i\text{Pr}_2)_2\}$ metal fragment stabilizes saturated d^6 -silyl derivatives, $\text{IrHCl}(\text{SiR}_3)\{\text{xant}(\text{P}^i\text{Pr}_2)_2\}$ and $\text{IrH}_2(\text{SiR}_3)\{\text{xant}(\text{P}^i\text{Pr}_2)_2\}$. The stabilization of saturated d^6 - $\text{Rh}\{\text{xant}(\text{P}^i\text{Pr}_2)_2\}$ species seems to need the presence of a coordinated π -donor ligand such as chloride.

EXPERIMENTAL SECTION

General Information. All reactions were carried out with rigorous exclusion of air using Schlenk-tube techniques. Solvents (except fluorobenzene that was dried and distilled under argon) were obtained oxygen- and water-free from an MBraun solvent purification apparatus. The alcohols used in the catalytic reactions were dried by standard procedures and distilled under argon prior to use. ¹H, ¹³C{¹H}, ³¹P{¹H}, and ²⁹Si{¹H} NMR spectra were recorded on Bruker 300 ARX, Bruker Avance 300 MHz and Bruker Avance 400 MHz instruments. Chemical shifts (expressed in parts per million) are referenced to residual solvent peaks (¹H, ¹³C{¹H}), external 85% H₃PO₄ (³¹P{¹H}), or external SiMe₄ (²⁹Si{¹H}). Coupling constants *J* and *N* are given in hertz. Attenuated total reflection infrared spectra (ATR-IR) of solid samples were run on a Perkin-Elmer Spectrum 100 FT-IR spectrometer. C, H, and N analyses were carried out in a Perkin-Elmer 2400 CHNS/O analyzer. High-resolution electrospray mass spectra were acquired using a MicroTOF-Q hybrid quadrupole time-of-flight spectrometer (Bruker Daltonics, Bremen, Germany).

$\text{Xant}(\text{P}^i\text{Pr}_2)_2$,² $\text{IrHCl}\{\text{xant}(\text{P}^i\text{Pr}_2)_2\}[\text{PrPCH}(\text{Me})\text{CH}_2]$ (**2**),⁶ $\text{RhCl}\{\text{xant}(\text{P}^i\text{Pr}_2)_2\}$ (**1**),⁶ $\text{RhH}\{\text{xant}(\text{P}^i\text{Pr}_2)_2\}$ (**8**),⁶ and $\text{NaBAR}^F_4 \cdot 2\text{H}_2\text{O}$ ²⁸ were prepared by published methods.

Reaction of $\text{RhCl}\{\text{xant}(\text{P}^i\text{Pr}_2)_2\}$ (1**) with H_2SiPh_2 : Preparation of $\text{RhHCl}(\text{SiHPh}_2)\{\text{xant}(\text{P}^i\text{Pr}_2)_2\}$ (**3**).** Diphenylsilane (109 μL , 0.57 mmol) was added to a solution of **1** (300 mg, 0.52 mmol) in toluene (3 mL). After the resulting solution was stirred for 10 min at room temperature, it was evaporated to dryness to afford a white residue. Addition of pentane afforded a white solid that was washed with pentane (2 \times 3 mL) and dried in vacuo. Yield: 320.0 mg (81%). Anal. Calcd. for $\text{C}_{39}\text{H}_{52}\text{ClOP}_2\text{RhSi}$: C, 61.21; H, 6.85. Found: C, 60.75; H, 6.72. HRMS (electrospray, *m/z*): calcd. for $\text{C}_{39}\text{H}_{52}\text{OP}_2\text{RhSi}$ [$\text{M} - \text{Cl}$]⁺: 729.2312; found: 729.2352. IR (neat compound, cm^{-1}): $\nu(\text{Rh}-\text{H})$ 2097 (w); $\nu(\text{Si}-\text{H})$ 2054 (m); $\nu(\text{C}-\text{O}-\text{C})$ 1093 (m). ¹H NMR (400.13 MHz, C_6D_6 , 293 K, δ): 8.35 (d, $J_{\text{H}-\text{H}} = 7.4$, 4H, CH SiHPh₂), 7.33 (t, $J_{\text{H}-\text{H}} = 7.4$, 4H, CH SiHPh₂), 7.21 (t, $J_{\text{H}-\text{H}} = 7.4$, 2H, CH SiHPh₂), 7.13 (d, $J_{\text{H}-\text{H}} = 7.6$, 2H, CH-arom), 7.07 (m, 2H, CH-arom), 6.88 (t, $J_{\text{H}-\text{H}} = 7.6$, 2H, CH-arom), 6.13 (t, $J_{\text{H}-\text{P}} = 11.2$, 1H, Si–H), 2.40 (m, 2H, PCH(CH₃)₂), 1.96 (m, 2H, PCH(CH₃)₂), 1.51 (dvt, $J_{\text{H}-\text{H}} = 7.2$, *N* = 14.4, 6H, PCH(CH₃)₂), 1.32 (s, 3H, CH₃), 1.24 (dvt, $J_{\text{H}-\text{H}} = 7.9$, *N* = 16.4, 6H, PCH(CH₃)₂), 1.20 (s, 3H, CH₃), 1.11 (dvt, $J_{\text{H}-\text{H}} = 7.6$, *N* = 15.8, 6H, PCH(CH₃)₂), 0.78 (dvt, $J_{\text{H}-\text{H}} = 6.5$, *N* =

12.9, 6H, PCH(CH₃)₂), -15.90 (dt, $J_{\text{H-Rh}} = 24.5$, $J_{\text{H-P}} = 14.2$, 1H, Rh-H). ¹³C{¹H} NMR (100.61 MHz, C₆D₆, 293 K, δ): 154.1 (vt, $N = 11.1$, C-arom), 142.9 (t, $J_{\text{C-P}} = 1.5$, C-arom, SiHPh₂), 137.2 (s, CH-arom SiHPh₂), 132.2 (vt, $N = 5.0$, C-arom), 131.1 (s, CH-arom SiHPh₂), 128.3 (s, CH-arom), 128.0 (s, CH-arom), 127.4 (s, CH-arom SiHPh₂), 124.0 (vt, $N = 5.2$, CH-arom), 123.1 (vt, $N = 26.5$, C-arom), 34.6 (s, C(CH₃)₂), 34.0, 28.7 (both s, C(CH₃)₂), 27.1 (vt, $N = 22.5$, PCH(CH₃)₂), 26.6 (dvt, $J_{\text{C-Rh}} = 2.3$, $N = 26.7$, PCH(CH₃)₂), 22.5 (s, PCH(CH₃)₂), 19.6 (s, PCH(CH₃)₂), 19.3 (vt, $N = 6.3$, PCH(CH₃)₂), 17.0 (s, PCH(CH₃)₂). ³¹P{¹H} NMR (161.98 MHz, C₆D₆, 293 K, δ): 42.9 (d, $J_{\text{P-Rh}} = 112$). ²⁹Si{¹H} NMR (59.63 MHz, C₆D₆, 293 K, δ): 4.1 (dt, $J_{\text{Si-Rh}} = 36$, $J_{\text{Si-P}} = 13$).

Reaction of RhCl{xant(PⁱPr)₂} (1) with HSiEt₃: Preparation of RhHCl(SiEt₃)xant(PⁱPr)₂ (4). Triethylsilane (42 μL, 0.25 mmol) was added to a solution of **1** (134 mg, 0.23 mmol) in toluene (3 mL). After the resulting solution was stirred for 1 h at room temperature, it was evaporated to dryness to afford a white residue. Addition of pentane afforded a white solid that was washed with pentane (2 × 1 mL) and dried in vacuo. Yield: 90.0 mg (56%). Anal. Calcd. for C₃₃H₅₆ClOP₂RhSi: C, 56.85; H, 8.10. Found: C, 56.80; H, 8.10. HRMS (electrospray, m/z): calcd. for C₃₃H₅₆OP₂RhSi [M - Cl]⁺: 661.2625; found: 661.2750. IR (cm⁻¹): ν(Rh-H) 2094 (w). ¹H NMR (400.13 MHz, C₆D₆, 293 K, δ): 7.20 (m, 2H, CH-arom), 7.11 (d, $J_{\text{H-H}} = 7.6$, 2H, CH-arom), 6.89 (t, $J_{\text{H-H}} = 7.6$, 2H, CH-arom), 2.86 (m, 2H, PCH(CH₃)₂), 2.20 (m, 2H, PCH(CH₃)₂), 1.57 (dvt, $J_{\text{H-H}} = 7.4$, $N = 15.6$, 6H, PCH(CH₃)₂), 1.45 (m, 6H, PCH(CH₃)₂ + 6H Si(CH₂CH₃)₃), 1.37 (t, $J_{\text{H-H}} = 6.8$, 9H, Si(CH₂CH₃)₃), 1.31 (s, 3H, CH₃), 1.20 (dvt, $J_{\text{H-H}} = 7.6$, $N = 16.8$, 6H, PCH(CH₃)₂), 1.18 (s, 3H, CH₃), 0.85 (dvt, $J_{\text{H-H}} = 6.6$, $N = 13.0$, 6H, PCH(CH₃)₂), -16.29 (dt, $J_{\text{H-Rh}} = 23.9$, $J_{\text{H-P}} = 15.7$, 1H, Rh-H). ¹³C{¹H} NMR (100.61 MHz, C₆D₆, 293 K, δ): 154.4 (vt, $N = 10.5$, C-arom), 132.2 (vt, $N = 4.2$, C-arom), 130.4 (s, CH-arom), 127.2 (s, CH-arom), 123.8 (s, CH-arom), 123.6 (vt, $N = 27.2$, C-arom), 34.6 (s, C(CH₃)₂), 32.7 (s, C(CH₃)₂), 28.0 (dvt, $J_{\text{C-Rh}} = 3.4$, $N = 26.0$, PCH(CH₃)₂), 27.9 (s, C(CH₃)₂), 27.6 (vt, $N = 19.6$, PCH(CH₃)₂), 20.3 (vt, $N = 4.4$, PCH(CH₃)₂), 20.1, 20.0, 17.7 (all s, PCH(CH₃)₂), 14.6 (s, Si(CH₂CH₃)₃), 10.1 (s, Si(CH₂CH₃)₃). ³¹P{¹H} NMR (161.98 MHz, C₆D₆, 293 K, δ): 41.6 (d, $J_{\text{P-Rh}} = 120$). ²⁹Si{¹H} NMR (59.63 MHz, C₆D₆, 293 K, δ): 40.3 (dt, $J_{\text{Si-Rh}} = 32$, $J_{\text{Si-P}} = 11$).

Reaction of 2 with H₂SiPh₂: Preparation of IrHCl(SiHPh₂)xant(PⁱPr)₂ (5). Diphenylsilane (37 μL, 0.20 mmol) was added to a solution of **2** (123 mg, 0.18 mmol) in toluene (1 mL). After the resulting solution was stirred for 2 h at room temperature, it was evaporated to dryness to afford a yellowish residue. Addition of pentane afforded a white solid that was washed with pentane (2 × 1 mL) and dried in vacuo. Yield: 65.0 mg (41%). Anal. Calcd. for C₃₉H₅₂ClIrOP₂Si: C, 54.82; H, 6.13. Found: C, 54.47; H, 5.98. HRMS (electrospray, m/z): calcd. for C₃₉H₅₁ClOP₂IrSi [M - H]⁺: 853.2490; found: 853.2422. IR (cm⁻¹): ν(Ir-H) 2223 (w); ν(Si-H) 2035 (w); ν(C-O-C) 1093 (m). ¹H NMR (300.08 MHz, C₆D₆, 293 K, δ): 8.32 (d, $J_{\text{H-H}} = 7.4$, 4H, CH SiHPh₂), 7.32 (t, $J_{\text{H-H}} = 7.4$, 4H, CH SiHPh₂), 7.19 (t, $J_{\text{H-H}} = 7.4$, 2H, CH SiHPh₂), 7.07 (m, 4H, CH-arom), 6.86 (t, $J_{\text{H-H}} = 7.5$, 2H, CH-arom), 6.02 (t, $J_{\text{H-P}} = 8.1$, 1H, Si-H), 2.59 (m, 2H, PCH(CH₃)₂), 2.07 (m, 2H, PCH(CH₃)₂), 1.43 (dvt, $J_{\text{H-H}} = 7.0$, $N = 14.3$, 6H, PCH(CH₃)₂), 1.32 (dvt, $J_{\text{H-H}} = 7.9$, $N = 16.3$, 6H, PCH(CH₃)₂), 1.27 (s, 3H, CH₃), 1.22 (s, 3H, CH₃), 1.09 (dvt, $J_{\text{H-H}} = 7.7$, $N = 16.2$, 6H, PCH(CH₃)₂), 0.80 (dvt, $J_{\text{H-H}} = 6.7$, $N = 13.5$, 6H, PCH(CH₃)₂), -19.91 (t, $J_{\text{H-P}} = 14.5$, 1H, Ir-H). ¹³C{¹H} NMR (75.46 MHz, C₆D₆, 293 K, δ): 154.5 (vt, $N = 9.7$, C-arom), 142.7 (s, C-arom, SiHPh₂), 137.2 (s, CH-arom SiHPh₂), 132.1 (vt, $N = 4.8$, C-arom), 131.4 (s, CH-arom SiHPh₂), 128.0 (s, CH-arom), 127.4 (s, CH-arom SiHPh₂), 125.1 (vt, $N = 32.6$, C-arom), 124.5 (vt, $N = 5.3$, CH-arom), 34.4 (s, C(CH₃)₂), 33.0, 30.8 (both s, C(CH₃)₂), 27.1 (vt, $N = 22.5$, PCH(CH₃)₂), 26.6 (vt, $N = 26.7$, PCH(CH₃)₂), 20.4, 19.5, 19.3, 17.6 (all s, PCH(CH₃)₂). ³¹P{¹H} NMR (121.49 MHz, C₆D₆, 293 K, δ): 29.9 (s). ²⁹Si{¹H} NMR (59.63 MHz, C₆D₆, 293 K, δ): -36.3 (t, $J_{\text{Si-P}} = 10$).

Reaction of 2 with HSiEt₃: Preparation of IrHCl(SiEt₃)xant(PⁱPr)₂ (6). Triethylsilane (27 μL, 0.16 mmol) was added to a solution of **2** (100 mg, 0.15 mmol) in toluene (3 mL). After the

resulting solution was stirred for 1 h at room temperature, it was evaporated to dryness to afford a white residue. Addition of pentane afforded a white solid that was washed with pentane (3 × 2 mL) and dried in vacuo. Yield: 80 mg (68%). Anal. Calcd. for C₃₃H₅₆ClIrOP₂Si: C, 50.39; H, 7.18. Found: C, 50.13; H, 7.36. HRMS (electrospray, m/z): calcd. for C₃₃H₅₆IrOP₂Si [M - Cl]⁺: 751.3200; found: 751.3231. IR (cm⁻¹): ν(Ir-H) 2227 (w). ¹H NMR (300.13 MHz, C₆D₆, 293 K, δ): 7.20 (m, 2H, CH-arom), 7.07 (dd, $J_{\text{H-H}} = 7.6$, $J_{\text{H-H}} = 1.5$, 2H, CH-arom), 6.87 (t, $J_{\text{H-H}} = 7.6$, 2H, CH-arom), 3.09 (m, 2H, PCH(CH₃)₂), 2.28 (m, 2H, PCH(CH₃)₂), 1.59 (dvt, $J_{\text{H-H}} = 7.3$, $N = 15.7$, 6H, PCH(CH₃)₂), 1.46-1.38 (m, 21H, 6H PCH(CH₃)₂ + 15H Si(CH₂CH₃)₃), 1.25 (s, 3H, CH₃), 1.21 (s, 3H, CH₃), 1.19 (dvt, $J_{\text{H-H}} = 7.4$, $N = 15.6$, 6H, PCH(CH₃)₂), 0.84 (dvt, $J_{\text{H-H}} = 6.9$, $N = 13.8$, 6H, PCH(CH₃)₂), -20.06 (t, $J_{\text{H-P}} = 16.0$, 1H, Ir-H). ¹³C{¹H} NMR (75.47 MHz, C₆D₆, 293 K, δ): 154.9 (vt, $N = 9.0$, C-arom), 132.5 (vt, $N = 4.8$, C-arom), 130.6 (s, CH-arom), 127.5 (s, CH-arom), 125.6 (vt, $N = 33.9$, C-arom), 124.4 (vt, $N = 4.5$, CH-arom), 34.5 (s, C(CH₃)₂), 31.3, 29.9 (both s, C(CH₃)₂), 28.8 (vt, $N = 32.3$, PCH(CH₃)₂), 28.3 (vt, $N = 22.9$, PCH(CH₃)₂), 20.5, 19.8, 19.7, 18.4 (all s, PCH(CH₃)₂), 13.2 (s, Si(CH₂CH₃)₃), 10.4 (s, Si(CH₂CH₃)₃). ³¹P{¹H} NMR (121.49 MHz, C₆D₆, 293 K, δ): 29.0 (s). ²⁹Si{¹H} NMR (59.63 MHz, C₆D₆, 293 K, δ): -7.6 (t, $J_{\text{Si-P}} = 8$).

Preparation of Rh(SiClPh₂)xant(PⁱPr)₂ (7). A Schlenk flask provided with a Teflon closure was charged with a solution of **3** (300 mg, 0.39 mmol) in toluene (3 mL) under argon atmosphere. After being stirred for 5 days at 50 °C (the reaction was periodically checked by ¹H and ³¹P{¹H} NMR spectroscopy) the resulting red solution was evaporated to dryness. Pentane was added to afford an orange solid, which was washed with pentane (2 × 3 mL) and dried in vacuo. Yield: 284 mg (95%). Anal. Calcd. for C₃₉H₅₀ClOP₂RhSi: C, 61.38; H, 6.60. Found: C, 61.52; H, 6.55. HRMS (electrospray, m/z) calcd. for C₃₉H₅₁ClOP₂RhSi: [M + H]⁺: 763.1922; found: 763.1936. IR (cm⁻¹): ν(C-O-C) 1091 (w). ¹H NMR (300.13 MHz, C₆D₆, 293 K, δ): 8.40 (d, $J_{\text{H-H}} = 7.3$, 4H, CH SiClPh₂), 7.33 (t, $J_{\text{H-H}} = 7.3$, 4H, CH SiClPh₂), 7.22 (t, $J_{\text{H-H}} = 7.3$, 2H, CH SiClPh₂), 7.16 (m, 2H, CH-arom), 7.08 (t, $J_{\text{H-H}} = 7.5$, 2H, CH-arom), 6.87 (t, $J_{\text{H-H}} = 7.5$, 2H, CH-arom), 2.27 (m, 4H, PCH(CH₃)₂), 1.24 (s, 6H, CH₃), 1.19 (dvt, $J_{\text{H-H}} = 7.7$, $N = 15.4$, 12H, PCH(CH₃)₂), 1.01 (dvt, $J_{\text{H-H}} = 7.2$, $N = 13.4$, 12H, PCH(CH₃)₂). ¹³C{¹H} NMR (75.46 MHz, C₆D₆, 293 K, δ): 155.7 (vt, $N = 13.6$, C-arom), 149.1 (dt, $J_{\text{C-Rh}} = 4.3$, $J_{\text{C-P}} = 1.6$, C-arom SiClPh₂), 137.2 (s, CH-arom SiClPh₂), 131.5 (vt, $N = 5.4$, C-arom), 131.4 (s, CH-arom), 127.4 (s, CH-arom), 127.3 (s, CH-arom SiClPh₂), 126.8 (s, CH-arom SiClPh₂), 124.5 (vt, $N = 15.0$, C-arom), 124.4 (vt, $N = 4.0$, CH-arom), 34.2 (s, C(CH₃)₂), 31.0 (s, C(CH₃)₂), 25.5 (dvt, $J_{\text{Rb-C}} = 2.9$, $N = 21.2$, PCH(CH₃)₂), 20.3 (vt, $N = 8.1$, PCH(CH₃)₂), 17.9 (s, PCH(CH₃)₂). ³¹P{¹H} NMR (121.49 MHz, C₆D₆, 293 K, δ): 49.4 (d, $J_{\text{P-Rh}} = 153.1$). ²⁹Si{¹H} NMR (59.63 MHz, C₆D₆, 293 K, δ): 49.2 (dt, $J_{\text{Si-Rh}} = 82$, $J_{\text{Si-P}} = 22$).

Isomerization of IrHCl(SiHPh₂)xant(PⁱPr)₂ (5) to IrH₂(SiClPh₂)xant(PⁱPr)₂ (9). **5** (100 mg, 0.11 mmol) was dissolved in toluene (3 mL) and heated at 50 °C for 48 h. After this time (the reaction was periodically checked by ¹H and ³¹P{¹H} NMR spectroscopy) the solution was evaporated to ca. 0.2 mL to afford a white residue. Addition of pentane afforded a white solid that was washed with pentane (1 × 1 mL) and dried in vacuo. Yield: 60 mg (60%). Anal. Calcd. for C₃₉H₅₂ClIrOP₂Si: C, 54.82; H, 6.13. Found: C, 54.85; H, 6.12. HRMS (electrospray, m/z): calcd. for C₃₉H₅₁ClIrOP₂Si [M - H]⁺: 853.2490; found: 853.2421. IR (cm⁻¹): ν(Ir-H) 2035 (w); ν(C-O-C) 1093 (m). ¹H NMR (300.08 MHz, C₆D₆, 293 K, δ): 8.37 (d, $J_{\text{H-H}} = 7.0$, 4H, CH SiClPh₂), 7.29 (t, $J_{\text{H-H}} = 7.0$, 4H, CH SiClPh₂), 7.18 (t, $J_{\text{H-H}} = 7.0$, 2H, CH SiClPh₂), 7.11 (m, 2H, CH-arom), 6.92 (dd, $J_{\text{H-H}} = 7.4$, $J_{\text{H-H}} = 1.3$, 2H, CH-arom), 6.86 (t, $J_{\text{H-H}} = 7.4$, 2H, CH-arom), 2.32 (m, 4H, PCH(CH₃)₂), 1.15 (dvt, $J_{\text{H-H}} = 7.3$, $N = 15.8$, 12H, PCH(CH₃)₂), 1.13 (s, 6H, CH₃), 1.08 (dvt, $J_{\text{H-H}} = 6.8$, $N = 14.2$, 12H, PCH(CH₃)₂), -4.90 (t, $J_{\text{H-P}} = 16.6$, 2H, Ir-H). ¹³C{¹H} NMR (75.46 MHz, C₆D₆, 293 K, δ): 156.9 (vt, $N = 10.4$, C-arom), 145.1 (s, C-arom SiClPh₂), 137.3 (s, CH-arom SiClPh₂), 132.4 (vt, $N = 5.1$, C-arom), 130.1 (s, CH-arom SiClPh₂), 128.2 (s, CH-arom), 126.6 (s, CH-arom), 126.5 (s, CH-arom SiClPh₂), 124.7 (vt, $N = 2.8$, CH-arom), 124.5 (vt, $N = 31.2$, C-arom), 34.4 (s, C(CH₃)₂),

29.4 (s, C(CH₃)₂), 24.6 (vt, *N* = 31.2, PCH(CH₃)₂), 18.9 (vt, *N* = 4.5, PCH(CH₃)₂), 17.7 (s, PCH(CH₃)₂). ³¹P{¹H} NMR (121.49 MHz, C₆D₆, 293 K, δ): 47.9 (s). ²⁹Si{¹H} NMR (59.63 MHz, C₆D₆, 293 K, δ): -4.8 (t, *J*_{Si-P} = 20).

Reaction of 6 with 2.0 equiv of H₂SiPh₂. In an NMR tube 6 (23.5 mg, 0.03 mmol) was dissolved in benzene-*d*₆ (0.4 mL), and diphenylsilane (11.5 μL, 0.06 mmol) was added. The tube was then immersed in an oil bath at 50 °C, and the reaction was monitored by ¹H and ³¹P{¹H} NMR spectroscopy. After 26 h, the ¹H and ³¹P{¹H} NMR spectra show signals corresponding to 6, 5, and 9 in a 50:26:24 molar ratio.

Reaction of RhH{xant(PⁱPr)₂}₂ (8) with HSiEt₃ at Low Temperature: Spectroscopic Detection of RhH₂{SiEt₃}xant(PⁱPr)₂ (10). A screw-top NMR tube containing a solution of 8 (26.7 mg, 0.05 mmol) in toluene-*d*₈ and cooled at 195 K was treated with HSiEt₃ (7.8 μL, 0.05 mmol). Immediately the NMR tube was introduced in a NMR probe precooled at 258 K. The immediate and quantitative conversion to RhH₂{SiEt₃}xant(PⁱPr)₂ (10) was observed by ¹H and ³¹P{¹H} NMR spectroscopies (in solution at this temperature 12 was observed as a minor product with time). ¹H NMR (400.13 MHz, C₇D₈, 258 K, δ): 7.06 (m, 2H, CH-arom), 6.93 (dd, *J*_{H-H} = 7.5, *J*_{H-H} = 1.2, 2H, CH-arom), 6.85 (t, *J*_{H-H} = 7.5, 2H, CH-arom), 2.44 (m, 4H, PCH(CH₃)₂), 1.46 (t, *J*_{H-H} = 7.7, 9H, Si(CH₂CH₃)₃), 1.32 (dvt, *J*_{H-H} = 8.4, *N* = 15.9, 12H, PCH(CH₃)₂), 1.24 (m, 6H, Si(CH₂CH₃)₃), 1.16 (s, 6H, CH₃), 1.10 (dvt, *J*_{H-H} = 6.7, *N* = 13.5, 12H, PCH(CH₃)₂), -5.63 (dt, *J*_{H-Rh} = 17.6, *J*_{H-P} = 18.0, 2H, RhH₂). ¹³C{¹H} NMR (100.62 MHz, C₇D₈, 258 K, δ): 156.8 (vt, *N* = 11.5, C-arom), 133.7 (vt, *N* = 4.7, C-arom), 129.0 (s, CH-arom), 125.0 (s, CH-arom), 123.5 (vt, *N* = 3.9, CH-arom), 122.7 (vt, *N* = 26.2, C-arom), 34.8 (s, C(CH₃)₂), 26.2 (br, C(CH₃)₂), 25.0 (s, PCH(CH₃)₂), 19.4 (vt, *N* = 7.9, PCH(CH₃)₂), 18.2 (br, PCH(CH₃)₂), 16.8 (s, Si(CH₂CH₃)₃), 10.7 (s, Si(CH₂CH₃)₃). ³¹P{¹H} NMR (161.98 MHz, C₇D₈, 258 K, δ): 61.6 (d, *J*_{P-Rh} = 126). ²⁹Si{¹H} NMR (79.49 MHz, C₇D₈, 258 K, δ): 33.0 (dt, *J*_{Si-Rh} = 33, *J*_{Si-P} = 9).

Reaction of RhH{xant(PⁱPr)₂}₂ (8) with HSiPh₃ at Low Temperature: Spectroscopic detection of RhH₂{SiPh₃}xant(PⁱPr)₂ (11). A solution of HSiPh₃ (12.9 mg, 0.05 mmol) in 0.5 mL of toluene-*d*₈ was added to a screw-top NMR tube containing 8 (27 mg, 0.05 mmol) and cooled at 195 K. Immediately the NMR tube was introduced into a NMR probe precooled at 258 K. The immediate and quantitative conversion to RhH₂{SiPh₃}xant(PⁱPr)₂ (11) was observed by ¹H and ³¹P{¹H} NMR spectroscopies (in solution at this temperature 13 was observed as a minor product with time). ¹H NMR (400.13 MHz, C₇D₈, 258 K, δ): 7.53 (d, *J*_{H-H} = 5.8, 6H, CH-arom), 7.27 (t, *J*_{H-H} = 7.2, 6H, CH-arom), 7.22 (m, 2H, CH-arom), 7.19 (d, *J*_{H-H} = 1.9, 3H, CH-arom), 6.95 (d, *J*_{H-H} = 7.5, 2H, CH-arom), 6.84 (t, *J*_{H-H} = 7.5, 2H, CH-arom), 2.08 (m, 4H, PCH(CH₃)₂), 1.24 (s, 6H, CH₃), 1.01 (dvt, *J*_{H-H} = 7.8, *N* = 15.4, 12H, PCH(CH₃)₂), 0.95 (dvt, *J*_{H-H} = 6.3, *N* = 14.1, 12H, PCH(CH₃)₂), -5.02 (dt, *J*_{H-Rh} = 19.3, *J*_{H-P} = 16.1, 2H, RhH₂). ¹³C{¹H} NMR (100.62 MHz, C₇D₈, 258 K, δ): 157.1 (vt, *N* = 11.4, C-arom), 148.9 (s, C-arom), 138.4 (s, CH-arom), 136.1 (s, CH-arom), 133.8 (vt, *N* = 4.3, C-arom), 130.0 (s, CH-arom), 129.3 (s, CH-arom), 128.3 (s, CH-arom), 123.9 (vt, *N* = 6.6, CH-arom), 122.9 (vt, *N* = 26.0, C-arom), 35.0 (s, C(CH₃)₂), 29.8 (s, C(CH₃)₂), 25.1 (vt, *N* = 19.7, PCH(CH₃)₂), 20.5, 17.7 (both s, PCH(CH₃)₂). ³¹P{¹H} NMR (161.98 MHz, C₇D₈, 258 K, δ): 59.3 (d, *J*_{P-Rh} = 120). ²⁹Si{¹H} NMR (79.49 MHz, C₇D₈, 258 K, δ): 9.4 (dt, *J*_{Si-Rh} = 42, *J*_{Si-P} = 12).

Reaction of RhH{xant(PⁱPr)₂}₂ (8) with HSiEt₃ at Room Temperature: Preparation of Rh{SiEt₃}xant(PⁱPr)₂ (12). Triethylsilane (33 μL, 0.20 mmol) was added to a solution of 8 (100.0 mg, 0.18 mmol) in toluene (3 mL). After the resulting solution was stirred for 5 min at room temperature, it was evaporated to dryness to afford a red residue. Addition of pentane afforded a red solid that was washed with pentane (2 × 0.5 mL) and dried in vacuo. Yield: 70.0 mg (58%). Anal. Calcd. for C₃₃H₅₅OP₂RhSi: C, 59.99; H, 8.39. Found: C, 59.90; H, 8.20. HRMS (electrospray, *m/z*): calcd. for C₃₃H₅₆OP₂RhSi [M + H]⁺: 661.2625; found: 661.2612. IR (cm⁻¹): ν(C-O-C) 1102 (m). ¹H NMR (400.13 MHz, C₆D₆, 293 K, δ): 7.33 (m, 2H, CH-arom), 7.12 (d, *J*_{H-H} = 7.5, 2H, CH-arom), 6.92 (t, *J*_{H-H}

= 7.5, 2H, CH-arom), 2.52 (m, 2H, PCH(CH₃)₂), 1.56 (t, *J*_{H-H} = 7.5, 9H, Si(CH₂CH₃)₃), 1.39 (m, 12H PCH(CH₃)₂ + 6H Si(CH₂CH₃)₃), 1.27 (s, 6H, CH₃), 1.10 (dvt, *J*_{H-H} = 6.7, *N* = 13.2, 12H, PCH(CH₃)₂). ¹³C{¹H} NMR (100.62 MHz, C₆D₆, 293 K, δ): 155.9 (vt, *N* = 13.6, C-arom), 131.8 (vt, *N* = 4.0, C-arom), 130.9 (s, CH-arom), 126.5 (s, CH-arom), 126.7 (vt, *N* = 12.5, C-arom), 123.9 (s, CH-arom), 34.4 (s, C(CH₃)₂), 30.4 (s, C(CH₃)₂), 26.6 (dvt, *J*_{C-Rh} = 3.3, *N* = 20.7, PCH(CH₃)₂), 20.6 (vt, *N* = 4.2, PCH(CH₃)₂), 18.5 (s, PCH(CH₃)₂), 13.7 (dt, *J*_{C-Rh} = 5.6, *J*_{C-P} = 3.2, Si(CH₂CH₃)₃), 11.1 (s, Si(CH₂CH₃)₃). ³¹P{¹H} NMR (161.98 MHz, C₆D₆, 293 K, δ): 46.0 (d, *J*_{P-Rh} = 171.3). ²⁹Si{¹H} NMR (59.63 MHz, C₆D₆, 293 K, δ): 25.0 (dt, *J*_{Si-Rh} = 54, *J*_{Si-P} = 19).

Reaction of RhH{xant(PⁱPr)₂}₂ (8) with HSiPh₃ at Room Temperature: Preparation of Rh{SiPh₃}xant(PⁱPr)₂ (13). Triphenylsilane (54.0 mg, 0.20 mmol) was added to a solution of 8 (100.0 mg, 0.18 mmol) in toluene (3 mL). After the resulting solution was stirred for 1 h at room temperature, it was evaporated to dryness to afford a dark residue. Addition of pentane afforded a red solid that was washed with pentane (2 × 1 mL) and dried in vacuo. Yield: 120.0 mg (81%). Anal. Calcd. for C₄₅H₅₅OP₂RhSi: C, 67.15; H, 6.89. Found: C, 66.76; H, 6.62. HRMS (electrospray, *m/z*): calcd. for C₄₅H₅₆OP₂RhSi [M + H]⁺: 805.2625; found: 805.2616. IR (cm⁻¹): ν(C-O-C) 1103 (m). ¹H NMR (300.13 MHz, C₆D₆, 293 K, δ): 8.38 (d, *J*_{H-H} = 8.2, 6H, CH SiPh₃), 7.30 (t, *J*_{H-H} = 7.5, 6H, CH SiPh₃), 7.21 (d, *J*_{H-H} = 7.5, 3H, CH SiPh₃), 7.20 (m, 2H, CH-arom), 7.12 (d, *J*_{H-H} = 7.6, 2H, CH-arom), 6.88 (t, *J*_{H-H} = 7.6, 2H, CH-arom), 1.63 (m, 4H, PCH(CH₃)₂), 1.28 (s, 6H, CH₃), 1.06 (dvt, *J*_{H-H} = 7.2, *N* = 16.6, 12H, PCH(CH₃)₂), 0.99 (dvt, *J*_{H-H} = 7.0, *N* = 13.0, 12H, PCH(CH₃)₂). ¹³C{¹H} NMR (75.46 MHz, C₆D₆, 293 K, δ): 155.9 (vt, *N* = 13.8, C-arom), 149.1 (dt, *J*_{C-Rh} = 2.7, *J*_{C-P} = 2.3, C-arom SiPh₃), 138.5 (s, CH-arom SiPh₃), 131.7 (vt, *N* = 5.1, C-arom), 131.2 (s, CH-arom), 126.8 (s, CH-arom SiPh₃), 126.7 (s, CH-arom), 126.6 (s, CH-arom SiPh₃), 125.6 (dvt, *J*_{C-Rh} = 1.8, *N* = 14.5, C-arom), 124.1 (vt, *N* = 3.5, CH-arom), 34.4 (s, C(CH₃)₂), 30.5 (s, C(CH₃)₂), 25.5 (dvt, *J*_{C-Rh} = 3.0, *N* = 19.4, PCH(CH₃)₂), 20.5 (vt, *N* = 8.4, PCH(CH₃)₂), 17.9 (s, PCH(CH₃)₂). ³¹P{¹H} NMR (121.50 MHz, C₆D₆, 293 K, δ): 44.7 (d, *J*_{P-Rh} = 159). ²⁹Si{¹H} NMR (59.63 MHz, C₆D₆, 293 K, δ): 14.4 (dt, *J*_{Si-Rh} = 66, *J*_{Si-P} = 21).

Reaction of Rh{SiClPh₂}xant(PⁱPr)₂ (7) with NaBAR₄·2H₂O: Preparation of [RhH{Si(OH)Ph₂}xant(PⁱPr)₂][BAR₄^F (14). Sodium tetrakis{3,5-bis(trifluoromethyl)phenyl}borate (NaBAR₄·2H₂O) (150 mg, 0.17 mmol) was added to a red solution of 7 (100 mg, 0.13 mmol) in fluorobenzene (3 mL). After being stirred for 1 h at room temperature, the resulting yellowish solution was evaporated to dryness, affording a yellowish residue. The addition of dichloromethane afforded a suspension that was filtered through Celite to remove the sodium salts. The solution thus obtained was evaporated to dryness. Addition of pentane afforded a white solid that was washed with pentane (3 × 1 mL) and dried in vacuo. Yield: 160.0 mg (76%). Anal. Calcd. for C₇₁H₆₄BF₂₄O₂P₂RhSi: C, 53.00; H, 4.00. Found: C, 53.40; H, 4.42. HRMS (electrospray, *m/z*): calcd. for C₃₉H₅₂O₂P₂RhSi [M]⁺: 745.2261; found: 745.2294. IR (cm⁻¹): ν(O-H) 3643 (w); ν(C-O-C) 1090 (m). ¹H NMR (300.13 MHz, CD₂Cl₂, 233 K, δ): 7.80–7.30 (m, 28H, CH-arom), 3.25 (s, 1H, OH), 2.49 (m, 4H, PCH(CH₃)₂), 1.91 (s, 3H, CH₃), 1.75 (m, 4H, PCH(CH₃)₂), 1.34 (m, 3H CH₃ + 6H PCH(CH₃)₂), 1.04 (m, 6H, PCH(CH₃)₂), 0.97 (m, 6H, PCH(CH₃)₂), 0.21 (m, 6H, PCH(CH₃)₂), -17.43 (dt, *J*_{H-Rh} = 39.4, *J*_{H-P} = 12.5, 1H, Rh-H). ¹³C{¹H} NMR (75.47 MHz, CD₂Cl₂, 233 K, δ): 162.2 (q, *J*_{C-B} = 49.9, C-B Ar₄^F), 157.8 (vt, *N* = 12.7, C-arom), 140.2 (dt, *J*_{C-Rh} = 1.3, *J*_{P-C} = 2.7, C-arom Si(OH)Ph), 135.2 (s, CH-arom Ar₄^F), 134.3 (vt, *N* = 5.7, C-arom), 131.4 (s, CH-arom Si(OH)Ph), 130.9 (s, CH-arom Si(OH)Ph), 130.4 (s, C-arom Ar₄^F), 129.7 (s, CH-arom), 129.3 (qq, *J*_{C-F} = 31.4, *J*_{C-B} = 2.9, C-CF₃ Ar₄^F), 128.3 (s, CH-arom Si(OH)Ph₂), 127.8 (vt, *N* = 5.5, CH-arom), 125.0 (q, *J*_{C-F} = 272, CF₃ Ar₄^F), 119.2 (vt, *N* = 25.6, C-arom), 117.9 (spt, *J*_{C-F} = 3.7, CH-arom Ar₄^F), 35.8 (s, C(CH₃)₂), 34.2 (s, C(CH₃)₂), 26.8 (vt, *N* = 27.4, PCH(CH₃)₂), 25.2 (s, C(CH₃)₂), 23.5 (vt, *N* = 18.8, PCH(CH₃)₂), 20.3, 20.0, 18.2, 17.0 (all s, PCH(CH₃)₂). ³¹P{¹H} NMR (121.50 MHz, CD₂Cl₂, 233 K, δ): 52.1 (d, *J*_{P-Rh} = 119).

$^{29}\text{Si}\{^1\text{H}\}$ NMR (59.63 MHz, CD_2Cl_2 , 233 K): δ 26.1 (dt, $J_{\text{Si-Rh}} = 32$, $J_{\text{Si-P}} = 7$).

Reactions of Alcoholysis of Diphenylsilane Catalyzed by $\text{RhH}\{\text{Si}(\text{OH})\text{Ph}_2\}\{\text{xant}(\text{P}^i\text{Pr}_2)_2\}\text{BAR}^F_4$ (14). In a typical procedure, the alcohol (except PhOH, that was dissolved in 200 μL of toluene) (1.57 mmol) was added via syringe to a solution of the catalyst (2.6×10^{-3} mmol), H_2SiPh_2 (1.57 mmol) in toluene (5 mL) placed into a 25 mL flask attached to a gas buret and immersed in a 32 °C bath, and the mixture was vigorously shaken (500 rpm) during the run. The reaction was monitored by measuring the volume of the evolved hydrogen with time until hydrogen evolution stopped. A representation of gas evolution versus time is included as Supporting Information. The solution was then passed through a column (silica gel) to remove the catalyst. Removal of the solvent gave the silyl ether. The product was analyzed by ^1H , $^{13}\text{C}\{^1\text{H}\}$, and $^{29}\text{Si}\{^1\text{H}\}$ NMR spectroscopy.

Spectroscopic Data of the Products of the Monoalcoholysis. $\text{HSi}(\text{OMe})\text{Ph}_2$. ^1H NMR (300.13 MHz, CDCl_3 , 293 K, δ): 7.58 (dd, $J_{\text{H-H}} = 7.6$, $J_{\text{H-H}} = 1.9$, 4H, CH-arom), 7.42–7.24 (m, 6H, CH-arom), 5.37 (s, 1H, Si-H), 3.54 (s, 3H, CH_3). $^{13}\text{C}\{^1\text{H}\}$ NMR (75.47 MHz, CDCl_3 , 293 K, δ): 134.8 (s, CH-arom), 133.8 (s, C-arom), 130.5 (s, CH-arom), 128.2 (s, CH-arom), 52.5 (s, O- CH_3). $^{29}\text{Si}\{^1\text{H}\}$ NMR (59.63 MHz, CDCl_3 , 293 K, δ): -14.5 (s).

$\text{HSi}(\text{OEt})\text{Ph}_2$. ^1H NMR (300.13 MHz, CDCl_3 , 293 K, δ): 7.62 (dd, $J_{\text{H-H}} = 7.7$, $J_{\text{H-H}} = 1.8$, 4H, CH-arom), 7.42–7.34 (m, 6H, CH-arom), 5.41 (s, 1H, Si-H), 3.84 (q, $J_{\text{H-H}} = 7.0$, 2H, CH_2), 1.24 (t, $J_{\text{H-H}} = 7.0$, 3H, CH_3). $^{13}\text{C}\{^1\text{H}\}$ NMR (75.47 MHz, CDCl_3 , 293 K, δ): 134.8 (s, CH-arom), 134.3 (s, C-arom), 130.4 (s, CH-arom), 128.1 (s, CH-arom), 60.7 (s, O- CH_2), 18.3 (s, CH_3). $^{29}\text{Si}\{^1\text{H}\}$ NMR (59.63 MHz, CDCl_3 , 293 K, δ): -17.6 (s).

$\text{HSi}(\text{O}^i\text{Bu})\text{Ph}_2$. ^1H NMR (400.13 MHz, CDCl_3 , 293 K, δ): 7.60 (dd, $J_{\text{H-H}} = 7.8$, $J_{\text{H-H}} = 1.7$, 4H, CH-arom), 7.39–7.32 (m, 6H, 2H, CH-arom), 5.40 (s, 1H, Si-H), 2.19 (t, $J_{\text{H-H}} = 6.5$, 2H, CH_2), 1.57 (m, 2H, CH_2), 1.36 (m, 2H, CH_2), 0.86 (t, $J_{\text{H-H}} = 7.4$, 3H, CH_3). $^{13}\text{C}\{^1\text{H}\}$ NMR (100.61 MHz, CDCl_3 , 293 K): δ 134.8 (s, CH-arom), 134.3 (s, C-arom), 130.4 (s, CH-arom), 128.1 (s, CH-arom), 64.7 (s, O- CH_2), 34.7 (s, CH_2), 19.1 (s, CH_2), 13.9 (s, CH_3). $^{29}\text{Si}\{^1\text{H}\}$ NMR (59.63 MHz, CDCl_3 , 293 K, δ): -17.4 (s).

$\text{HSi}(\text{O}^n\text{Octyl})\text{Ph}_2$. ^1H NMR (400.13 MHz, CDCl_3 , 293 K, δ): 7.61 (dd, $J_{\text{H-H}} = 7.8$, $J_{\text{H-H}} = 1.6$, 4H, CH-arom), 7.40–7.33 (m, 6H, CH-arom), 5.40 (s, 1H, Si-H), 3.75 (t, $J_{\text{H-H}} = 6.4$, 2H, CH_2), 1.58 (m, 2H, CH_2), 1.35–1.15 (m, 10H, CH_2), 0.86 (t, $J_{\text{H-H}} = 6.7$, 3H, CH_3). $^{13}\text{C}\{^1\text{H}\}$ NMR (100.61 MHz, CDCl_3 , 293 K, δ): 134.8 (s, CH-arom), 134.3 (s, C-arom), 130.4 (s, CH-arom), 128.1 (s, CH-arom), 65.1 (s, O- CH_2), 32.5, 32.0, 29.4, 25.9, 22.8 (all s, CH_2), 14.3 (s, CH_3). $^{29}\text{Si}\{^1\text{H}\}$ NMR (59.63 MHz, CDCl_3 , 293 K, δ): -17.4 (s).

$\text{HSi}(\text{OCH}_2\text{Ph})\text{Ph}_2$. ^1H NMR (400.13 MHz, CDCl_3 , 293 K, δ): 7.62 (dd, $J_{\text{H-H}} = 7.9$, $J_{\text{H-H}} = 1.5$, 4H, CH-arom), 7.41–7.28 (m, 11H, CH-arom), 5.47 (s, 1H, Si-H), 4.83 (s, 2H, CH_2). $^{13}\text{C}\{^1\text{H}\}$ NMR (100.61 MHz, CDCl_3 , 293 K, δ): 140.2 (s, C-arom), 134.8 (s, CH-arom), 133.8 (s, C-arom), 130.6, 128.4, 128.2, 127.4, 126.9 (all s, CH-arom), 66.7 (s, CH_2). $^{29}\text{Si}\{^1\text{H}\}$ NMR (59.63 MHz, CDCl_3 , 293 K, δ): -16.1 (s).

$\text{HSi}(\text{O}^i\text{Pr})\text{Ph}_2$. ^1H NMR (300.13 MHz, CDCl_3 , 293 K): δ 7.60 (dd, $J_{\text{H-H}} = 7.6$, $J_{\text{H-H}} = 1.9$, 4H, CH-arom), 7.43–7.29 (m, 6H, CH-arom), 5.44 (s, 1H, Si-H), 4.15 (sept, $J_{\text{H-H}} = 6.1$, 1H, CH), 1.21 (d, $J_{\text{H-H}} = 6.1$, 6H, CH_3). $^{13}\text{C}\{^1\text{H}\}$ NMR (75.47 MHz, CDCl_3 , 293 K): δ 135.0 (s, C-arom), 134.8 (s, CH-arom), 130.3 (s, CH-arom), 128.1 (s, CH-arom), 67.5 (s, O-CH), 25.4 (s, CH_3). $^{29}\text{Si}\{^1\text{H}\}$ NMR (59.63 MHz, CDCl_3 , 293 K, δ): -20.5 (s).

$\text{HSi}(\text{OCy})\text{Ph}_2$. ^1H NMR (400.13 MHz, CDCl_3 , 293 K, δ): 7.61 (dd, $J_{\text{H-H}} = 7.8$, $J_{\text{H-H}} = 1.7$, 4H, CH-arom), 7.39–7.31 (m, 6H, CH-arom), 5.38 (s, 1H, Si-H), 3.72 (m, 1H, CH), 1.57, 1.77–1.11 (m, 10H, CH_2). $^{13}\text{C}\{^1\text{H}\}$ NMR (100.61 MHz, CDCl_3 , 293 K, δ): 135.0 (s, C-arom), 134.7 (s, CH-arom), 130.3 (s, CH-arom), 128.1 (s, CH-arom), 73.1 (s, O-CH), 35.4, 25.7, 24.2 (all s, CH_2). $^{29}\text{Si}\{^1\text{H}\}$ NMR (59.63 MHz, CDCl_3 , 293 K, δ): -20.9 (s).

$\text{HSi}(\text{O}^t\text{Bu})\text{Ph}_2$. ^1H NMR (400.13 MHz, CDCl_3 , 293 K, δ): 7.60 (dd, $J_{\text{H-H}} = 7.7$, $J_{\text{H-H}} = 1.8$, 4H, CH-arom), 7.40–7.30 (m, 6H, CH-arom), 5.55 (s, 1H, Si-H), 1.31 (s, 9H, CH_3). $^{13}\text{C}\{^1\text{H}\}$ NMR (100.61 MHz, CDCl_3 , 293 K, δ): 136.2 (s, C-arom), 134.6, 130.0, 128.0 (all s, CH-

arom), 73.8 (s, O-C), 31.7 (s, CH_3). $^{29}\text{Si}\{^1\text{H}\}$ NMR (59.63 MHz, CDCl_3 , 293 K, δ): -29.5 (s).

$\text{HSi}(\text{O}^n\text{Ph})\text{Ph}_2$. ^1H NMR (400.13 MHz, CDCl_3 , 293 K, δ): 7.65 (d, $J_{\text{H-H}} = 6.4$, 4H, CH-arom), 7.41–7.28 (m, 7H, CH-arom), 7.18–7.12 (m, 2H, CH-arom), 6.92 (m, 2H, CH-arom), 5.72 (s, 1H, Si-H). $^{13}\text{C}\{^1\text{H}\}$ NMR (100.61 MHz, CDCl_3 , 293 K, δ): 155.5 (s, C-arom), 134.8 (s, CH-arom), 133.0 (s, C-arom), 130.8 (s, C-arom), 129.8 (s, CH-arom), 128.3 (s, CH-arom), 122.0 (s, CH-arom), 119.4 (s, CH-arom). $^{29}\text{Si}\{^1\text{H}\}$ NMR (59.63 MHz, CDCl_3 , 293 K, δ): -19.8 (s).

Structural Analysis of Complexes 3, 6, 7, 9, 12, and 14.

Crystals suitable for the X-ray diffraction were obtained by slow diffusion of pentane into solutions of 3 and 6 in toluene, of diethyl ether into solutions of 14 in dichloromethane, and by slow evaporation of benzene (7) or pentane (9 and 12). X-ray data were collected on a Bruker Smart APEX (3, 6, 7) and Bruker Apex II CCD (9, 12, 14) diffractometers equipped with a normal focus, 2.4 kW sealed tube source (Mo radiation, $\lambda = 0.71073 \text{ \AA}$) operating at 50 kV and 30 (7, 12) or 40 (3, 6, 9, 14) mA. Data were collected over the complete sphere by a combination of four sets. Each frame exposure time was 10 s (7, 14), 20 s (3, 6), 30 s (9), or 40 s (12) covering 0.3° in ω . Data were corrected for absorption by using a multiscan method applied with the SADABS program.²⁹ The structures were solved by the Patterson (Rh atom of 3, 7, 12, and 14, and Ir atoms of 6 and 9) or direct methods and conventional Fourier techniques and refined by full-matrix least-squares on F^2 with SHELXL97.³⁰ Anisotropic parameters were used in the last cycles of refinement for all non-hydrogen atoms. The hydrogen atoms were observed or calculated and refined freely or using a restricted riding model. Hydride ligands were observed in the difference Fourier maps but refined with restrained bond length. One of the benzene crystallization molecules of 7 and two of the CF_3 groups of the BAR^F_4 anion of 14 were found to be disordered. These disordered atoms were refined isotropically with restrained geometry. For all structures, the highest electronic residuals were observed in the close proximity of the metal centers and make no chemical sense.

Crystal Data for 3. $\text{C}_{39}\text{H}_{52}\text{ClOP}_2\text{RhSi} \cdot 0.5\text{C}_7\text{H}_8$, M_w 811.26, colorless, prism (0.15 \times 0.13 \times 0.09), monoclinic, space group $\text{C2}/c$, a : 31.6766(18) \AA , b : 11.6863(7) \AA , c : 22.6325(13) \AA , $\beta = 107.2060(10)^\circ$, $V = 8003.2(8) \text{ \AA}^3$, $Z = 8$, D_{calc} : 1.347 g cm^{-3} , $F(000)$: 3400, $T = 100(2) \text{ K}$, μ 0.635 mm^{-1} . 39319 measured reflections (2θ : 4–57°, ω scans 0.3°), 9550 unique ($R_{\text{int}} = 0.0454$); minimum/maximum transmission factors 0.748/0.862. Final agreement factors were $R^1 = 0.0471$ (7392 observed reflections, $I > 2\sigma(I)$) and $wR^2 = 0.1203$; data/restraints/parameters 9550/0/436; GOF = 1.056. Largest peak and hole 1.683 and -0.504 $\text{e}/\text{ \AA}^3$.

Crystal Data for 6. $\text{C}_{33}\text{H}_{56}\text{ClIrOP}_2\text{Si}$, M_w 786.46, colorless, prism (0.18 \times 0.07 \times 0.06), monoclinic, space group $\text{C2}/c$, a : 38.867(3) \AA , b : 9.4817(8) \AA , c : 18.9847(16) \AA , $\beta = 90.5580(10)^\circ$, $V = 6995.9(10) \text{ \AA}^3$, $Z = 8$, D_{calc} : 1.493 g cm^{-3} , $F(000)$: 3200, $T = 100(2) \text{ K}$, μ 0.403 mm^{-1} . 31 121 measured reflections (2θ : 4–57°, ω scans 0.3°), 8313 unique ($R_{\text{int}} = 0.0428$); minimum/maximum transmission factors 0.582/0.862. Final agreement factors were $R^1 = 0.0441$ (7026 observed reflections, $I > 2\sigma(I)$) and $wR^2 = 0.1140$; data/restraints/parameters 8313/1/368; GOF = 1.064. Largest peak and hole 4.199 and -2.541 $\text{e}/\text{ \AA}^3$.

Crystal Data for 7. $\text{C}_{39}\text{H}_{50}\text{ClOP}_2\text{RhSi} \cdot 2\text{C}_6\text{H}_6$, M_w 919.40, red, prism (0.22 \times 0.13 \times 0.09), triclinic, space group $\text{P}\bar{1}$, a : 10.2599(7) \AA , b : 11.9553(8) \AA , c : 20.3304(14) \AA , $\alpha = 77.8960(10)^\circ$, $\beta = 84.2760(10)^\circ$, $\gamma = 71.9240(10)^\circ$, $V = 2316.3(3) \text{ \AA}^3$, $Z = 2$, D_{calc} : 1.318 g cm^{-3} , $F(000)$: 964, $T = 120(2) \text{ K}$, μ 0.557 mm^{-1} . 27059 measured reflections (2θ : 2–57°, ω scans 0.3°), 10623 unique ($R_{\text{int}} = 0.0386$); minimum/maximum transmission factors 0.642/0.862. Final agreement factors were $R^1 = 0.0460$ (8775 observed reflections, $I > 2\sigma(I)$) and $wR^2 = 0.0940$; data/restraints/parameters 10623/0/488; GOF = 1.071. Largest peak and hole 0.747 and -0.793 $\text{e}/\text{ \AA}^3$.

Crystal Data for 9. $\text{C}_{39}\text{H}_{52}\text{ClIrOP}_2\text{Si} \cdot 1/4(\text{C}_5\text{H}_{12})$, M_w 872.52, colorless, irregular prism (0.16 \times 0.14 \times 0.10), monoclinic, space group $\text{C2}/c$, a : 23.228(3) \AA , b : 23.110(3) \AA , c : 17.543(2) \AA , $\beta = 122.110(2)^\circ$, $V = 7976.6(16) \text{ \AA}^3$, $Z = 8$, D_{calc} : 1.453 g cm^{-3} , $F(000)$: 3540, $T = 100(2) \text{ K}$, μ 3.554 mm^{-1} . 43 448 measured reflections (2θ :

2–59°, ω scans 0.3°), 10458 unique ($R_{\text{int}} = 0.0488$); minimum/maximum transmission factors 0.487/0.704. Final agreement factors were $R^1 = 0.0323$ (7537 observed reflections, $I > 2\sigma(I)$) and $wR^2 = 0.0804$; data/restraints/parameters 10458/5/435; GOF = 0.941. Largest peak and hole 2.390 and $-1.020 \text{ e}/\text{\AA}^3$.

Crystal Data for 12. $\text{C}_{33}\text{H}_{55}\text{OP}_2\text{RhSi}$, M_{w} 660.71, dark red, prism ($0.17 \times 0.12 \times 0.07$), orthorhombic, space group $P2(1)2(1)2(1)$, a : 8.5450(9) Å, b : 18.3095(19) Å, c : 22.353(2) Å, $V = 3497.3(6) \text{ \AA}^3$, $Z = 4$, D_{calc} : 1.255 g cm^{-3} , $F(000)$: 1400, $T = 100(2) \text{ K}$, μ 0.637 mm^{-1} . 37 385 measured reflections (2θ : 3–59°, ω scans 0.3°), 9055 unique ($R_{\text{int}} = 0.0629$); minimum/maximum transmission factors 0.747/0.944. Final agreement factors were $R^1 = 0.0337$ (7333 observed reflections, $I > 2\sigma(I)$) and $wR^2 = 0.0665$; Flack parameter 0.44(2); data/restraints/parameters 9055/0/357; GOF = 0.955. Largest peak and hole 1.056 and $-0.457 \text{ e}/\text{\AA}^3$.

Crystal Data for 14. $\text{C}_{71}\text{H}_{64}\text{BF}_{24}\text{O}_2\text{P}_2\text{RhSi-OC}_4\text{H}_{10}$, M_{w} 1683.09, colorless, prism ($0.23 \times 0.22 \times 0.17$), triclinic, space group $P\bar{1}$, a : 10.1457(10) Å, b : 19.559(2) Å, c : 19.979(2) Å, $\alpha = 87.073(2)^\circ$, $\beta = 88.661(2)^\circ$, $\gamma = 77.015(2)^\circ$, $V = 3858.0(7) \text{ \AA}^3$, $Z = 2$, D_{calc} : 1.449 g cm^{-3} , $F(000)$: 1716, $T = 100(2) \text{ K}$, μ 0.382 mm^{-1} . 42965 measured reflections (2θ : 3–59°, ω scans 0.3°), 19600 unique ($R_{\text{int}} = 0.0360$); minimum/maximum transmission factors 0.778/0.944. Final agreement factors were $R^1 = 0.0498$ (14559 observed reflections, $I > 2\sigma(I)$) and $wR^2 = 0.1389$; data/restraints/parameters 19600/18/978; GOF = 1.062. Largest peak and hole 1.491 and $-0.839 \text{ e}/\text{\AA}^3$.

■ ASSOCIATED CONTENT

■ Supporting Information

CIF files giving positional and displacement parameters, crystallographic data, and bond lengths and angles of compounds **3**, **6**, **7**, **9**, **12**, and **14**. NMR spectra of complexes **10** and **11** and a plot of hydrogen evolution versus time for the monoalcoholysis of diphenylsilane catalyzed by complex **14**. This material is available free of charge via the Internet at <http://pubs.acs.org>.

■ AUTHOR INFORMATION

Corresponding Author

*E-mail: maester@unizar.es.

Notes

The authors declare no competing financial interest.

■ ACKNOWLEDGMENTS

Financial support from the MINECO of Spain (Projects CTQ2011-23459 and Consolider Ingenio 2010 CSD2007-00006), the Diputación General de Aragón (E-35), FEDER, and the European Social Fund is acknowledged. We are very grateful to Dr. Enrique Oñate for collecting the X-ray diffraction data.

■ REFERENCES

- (1) (a) Albrecht, M.; van Koten, G. *Angew. Chem., Int. Ed.* **2001**, *40*, 3750. (b) van der Boom, M. E.; Milstein, D. *Chem. Rev.* **2003**, *103*, 1759. (c) Singleton, J. T. *Tetrahedron* **2003**, *59*, 1837. (d) *The Chemistry of Pincer Compounds*; Morales-Morales, D.; Jensen, C. M., Eds.; Elsevier Science: Amsterdam: The Netherlands, 2007. (e) Benito-Garagorri, D.; Kirchner, K. *Acc. Chem. Res.* **2008**, *41*, 201. (f) Whited, M. T.; Grubbs, R. H. *Acc. Chem. Res.* **2009**, *42*, 1607. (g) Choi, J.; MacArthur, A. H. R.; Brookhart, M.; Goldman, A. S. *Chem. Rev.* **2011**, *111*, 1761. (h) Haibach, M. C.; Kundu, S.; Brookhart, M.; Goldman, A. S. *Acc. Chem. Res.* **2012**, *45*, 947.
- (2) Asensio, G.; Cuenca, A. B.; Esteruelas, M. A.; Medio-Simón, M.; Oliván, M.; Valencia, M. *Inorg. Chem.* **2010**, *49*, 8665.
- (3) Esteruelas, M. A.; Honczek, N.; Oliván, M.; Oñate, E.; Valencia, M. *Organometallics* **2011**, *30*, 2468.

(4) Alós, J.; Bolaño, T.; Esteruelas, M. A.; Oliván, M.; Oñate, E.; Valencia, M. *Inorg. Chem.* **2013**, *52*, 6199.

(5) Recent findings on Rh(POP) chemistry: (a) Goldman and co-workers have described the synthesis and reactivity of related rhodium complexes with $\text{xant}(\text{P}^t\text{Bu}_2)_2$ and 2,5-bis((di-*tert*-butylphosphino)methyl)furan. See: Haibach, M. C.; Wang, D. Y.; Emge, T. J.; Krogh-Jespersen, K.; Goldman, A. S. *Chem. Sci.* **2013**, *4*, 3683. (b) Weller and co-workers have reported on the hydroacylation of alkynes catalyzed by Rh-DPEphos complexes. See: Pawley, R. J.; Huertos, M. A.; Lloyd-Jones, G. C.; Weller, A. S.; Willis, M. C. *Organometallics* **2012**, *31*, S650. (c) Haynes and co-workers have isolated an acetyl-Rh-xantphos complex during the study of the mechanism of methanol carbonylation. See: Williams, G. L.; Parks, C. M.; Smith, C. R.; Adams, H.; Haynes, A.; Meijer, A. J. H. M.; Sunley, G. J.; Gaemers, S. *Organometallics* **2011**, *30*, 6166. (d) Julian and Hartwig have discovered a Rh-POP catalyst for the intramolecular hydroamination of aminoalkenes. See: Julian, L. D.; Hartwig, J. F. *J. Am. Chem. Soc.* **2010**, *132*, 13183.

(6) Esteruelas, M. A.; Oliván, M.; Vélez, A. *Inorg. Chem.* **2013**, *52*, 5339.

(7) Corey, J. Y. *Chem. Rev.* **2011**, *111*, 863.

(8) (a) Roy, A. K. *Adv. Organomet. Chem.* **2008**, *55*, 1. (b) Normand, A. T.; Cavell, K. J. *Eur. J. Inorg. Chem.* **2008**, 2781. (c) Troegel, D.; Stohrer, J. *Coord. Chem. Rev.* **2011**, *255*, 1440.

(9) See for example: (a) Esteruelas, M. A.; Herrero, J.; López, F. M.; Martín, M.; Oro, L. A. *Organometallics* **1999**, *18*, 1110. (b) Díaz, J.; Esteruelas, M. A.; Herrero, J.; Moralejo, L.; Oliván, M. J. *Catal.* **2000**, *195*, 187. (c) Esteruelas, M. A.; Herrero, J.; Oliván, M. *Organometallics* **2004**, *23*, 3891. (d) Yang, J.; Brookhart, M. J. *Am. Chem. Soc.* **2007**, *129*, 12656. (e) Yang, J.; Brookhart, M. *Adv. Synth. Catal.* **2009**, *351*, 175.

(10) See for example: (a) Goikhman, R.; Aizenberg, M.; Shimon, L. J. W.; Milstein, D. *J. Am. Chem. Soc.* **1996**, *118*, 10894. (b) Field, L. D.; Messerle, B. A.; Rehr, M.; Soler, L. P.; Hambley, T. W. *Organometallics* **2003**, *22*, 2387. (c) Chandrasekhar, V.; Boomishankar, R.; Nagendran, S. *Chem. Rev.* **2004**, *104*, 5847. (d) Muraoka, T.; Abe, K.; Haga, Y.; Nakamura, T.; Ueno, K. *J. Am. Chem. Soc.* **2011**, *133*, 15365.

(11) (a) Yang, J.; White, P. S.; Schauer, C. K.; Brookhart, M. *Angew. Chem., Int. Ed.* **2008**, *47*, 4141. (b) Yang, J.; White, P. S.; Brookhart, M. *J. Am. Chem. Soc.* **2008**, *130*, 17509. (c) Park, S.; Brookhart, M. *J. Am. Chem. Soc.* **2012**, *134*, 640.

(12) (a) Calimano, E.; Tilley, T. D. *J. Am. Chem. Soc.* **2008**, *130*, 9226. (b) Calimano, E.; Tilley, T. D. *J. Am. Chem. Soc.* **2009**, *131*, 11161. (c) Calimano, E.; Tilley, T. D. *Organometallics* **2010**, *29*, 1680. (d) Calimano, E.; Tilley, T. D. *Dalton Trans.* **2010**, 39, 9250.

(13) Gatard, S.; Chen, C.-H.; Foxman, B. M.; Ozerov, O. V. *Organometallics* **2008**, *27*, 6257.

(14) Goikhman, R.; Aizenberg, M.; Ben-David, Y.; Shimon, L. J. W.; Milstein, D. *Organometallics* **2002**, *21*, 5060.

(15) (a) Johnson, C. E.; Eisenberg, R. *J. Am. Chem. Soc.* **1985**, *107*, 6531. (b) Esteruelas, M. A.; Lahoz, F. J.; Oliván, M.; Oñate, E.; Oro, L. A. *Organometallics* **1995**, *14*, 3486. (c) Esteruelas, M. A.; Oliván, M.; Oro, L. A. *Organometallics* **1996**, *15*, 814.

(16) See for example: (a) Osakada, K.; Koizumi, T.; Yamamoto, T. *Organometallics* **1997**, *16*, 2063. (b) Osakada, K.; Sarai, S.; Koizumi, T.; Yamamoto, T. *Organometallics* **1997**, *16*, 3973. (c) Turculet, L.; Feldman, J. D.; Tilley, T. D. *Organometallics* **2004**, *23*, 2488. (d) McBee, J. L.; Tilley, T. D. *Organometallics* **2009**, *28*, 5072. (e) Hoffmann, F.; Wagler, J.; Böhme, U.; Roewer, G. *J. Organomet. Chem.* **2012**, *705*, 59.

(17) Esteruelas, M. A.; Oro, L. A. *Coord. Chem. Rev.* **1999**, *193–195*, 557.

(18) See for example: (a) Fernández, M. J.; Esteruelas, M. A.; Covarrubias, M.; Oro, L. A.; Apreada, M.-C.; Foces-Foces, C.; Cano, F. H. *Organometallics* **1989**, *8*, 1158. (b) Esteruelas, M. A.; Lahoz, F. J.; Oñate, E.; Oro, L. A.; Rodríguez, L. *Organometallics* **1996**, *15*, 823. (c) Vicent, C.; Viciano, M.; Mas-Marzá, E.; Sanaú, M.; Peris, E. *Organometallics* **2006**, *25*, 3713. (d) Sangtrirutnugul, P.; Tilley, T. D.

Organometallics **2007**, *26*, 5557. (e) Bleeke, J. R.; Thananathanachon, T.; Rath, N. P. *Organometallics* **2008**, *27*, 2436.

(19) Square-planar rhodium(I)-silyl complexes are somewhat rare: (a) Thorn, D.; Harlow, R. L. *Inorg. Chem.* **1990**, *29*, 2017. (b) Aizenberg, M.; Milstein, D. *Science* **1994**, *265*, 359. (c) Hoffmann, P.; Meier, C.; Hiller, W.; Heckel, M.; Riede, J.; Schmidt, U. *J. Organomet. Chem.* **1995**, *490*, 51. (d) Mitchell, G. P.; Tilley, T. D.; Yap, G. P. A.; Rheingold, A. L. *Organometallics* **1995**, *14*, 5472. (e) Aizenberg, M.; Ott, J.; Elsevier, C. J.; Milstein, D. *J. Organomet. Chem.* **1998**, *551*, 81.

(20) Hendriksen, D. E.; Oswald, A. A.; Ansell, G. B.; Leta, S.; Kastrup, R. V. *Organometallics* **1989**, *8*, 1153.

(21) See for example: (a) van der Veen, L. A.; Keever, P. H.; Schoemaker, G. C.; Reek, J. N. H.; Kamer, P. C. J.; van Leeuwen, P. W. N. M.; Lutz, M.; Spek, A. L. *Organometallics* **2000**, *19*, 872. (b) Fox, D. J.; Duckett, S. B.; Flaschenriem, C.; Brennessel, W. W.; Schneider, J.; Gunay, A.; Eisenberg, R. *Inorg. Chem.* **2006**, *45*, 7197. (c) Marimuthu, T.; Bala, M. D.; Friedrich, H. B. *J. Coord. Chem.* **2009**, *62*, 1407. (d) Jian, Y.; Peng, S.; Li, X.; Wen, X.; He, J.; Jiang, L.; Dang, Y. *Inorg. Chim. Acta* **2011**, *368*, 37. (e) Pontiggia, A. J.; Chaplin, A. B.; Weller, A. S. *J. Organomet. Chem.* **2011**, *696*, 2870.

(22) (a) Bolaño, T.; Castarlenas, R.; Esteruelas, M. A.; Oñate, E. *J. Am. Chem. Soc.* **2007**, *129*, 8850.

(23) Hübler, K.; Hunt, P. A.; Maddock, S. M.; Rickard, C. E. F.; Roper, W. R.; Salter, D. M.; Schwerdtfeger, P.; Wright, L. J. *Organometallics* **1997**, *16*, 5076.

(24) Findlater, M.; Bernskoetter, W. H.; Brookhart, M. *J. Am. Chem. Soc.* **2010**, *132*, 4534.

(25) See for example: (a) Luo, X. L.; Crabtree, R. H. *J. Am. Chem. Soc.* **1989**, *111*, 2527. (b) Doyle, M. P.; High, K. G.; Bagheri, V.; Pieters, R. J.; Lewis, P. J.; Pearson, M. M. *J. Org. Chem.* **1990**, *55*, 6082. (c) Barber, D. E.; Lu, Z.; Richardson, T.; Crabtree, R. H. *Inorg. Chem.* **1992**, *31*, 4709. (d) Chang, S.; Scharer, E.; Brookhart, M. *J. Mol. Catal. A: Chem.* **1998**, *130*, 107.

(26) Werner, H. *Angew. Chem., Int. Ed. Engl.* **1983**, *22*, 927.

(27) (a) Kim, S.; Chang, H. *Bull. Chem. Soc. Jpn.* **1985**, *58*, 3669. (b) D'Sa, B. A.; McLeod, D.; Verkade, J. G. *J. Org. Chem.* **1997**, *62*, 5057.

(28) Brookhart, M.; Grant, B.; Volpe, A. F., Jr. *Organometallics* **1992**, *11*, 3920.

(29) Blessing, R. H. *Acta Crystallogr.* **1995**, *A51*, 33. SADABS: Area-detector absorption correction; Bruker-AXS: Madison, WI, 1996.

(30) SHELXTL, Package v. 6.10; Bruker-AXS: Madison, WI, 2000. Sheldrick, G. M. *Acta Crystallogr.* **2008**, *A64*, 112.